The Impulsive Heating Rate in Shocked O Star Winds:

Determined Directly from High-Resolution X-ray Spectra

David Cohen
Department of Physics & Astronomy
Swarthmore College

Zack Li (Swarthmore ’16), Jon Sundqvist and Stan Owocki (Delaware), Véronique Petit (Florida Institute of Technology), Maurice Leutenegger (GSFC), Marc Gagné (West Chester), Asif ud-Doula (Penn St.)

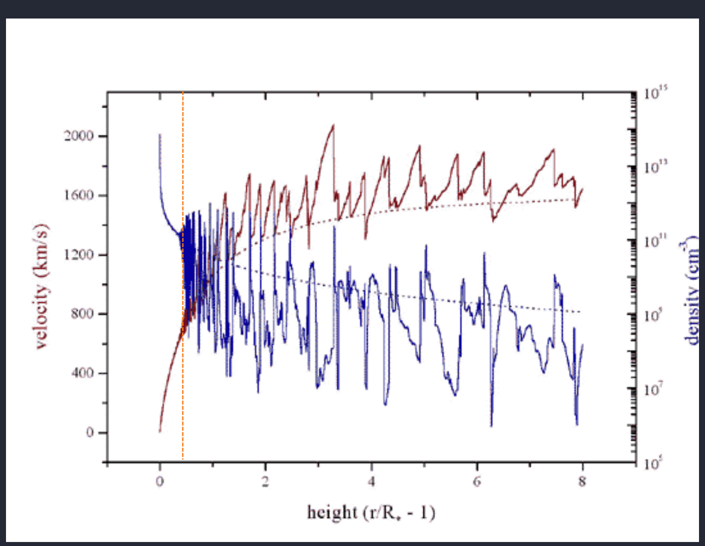

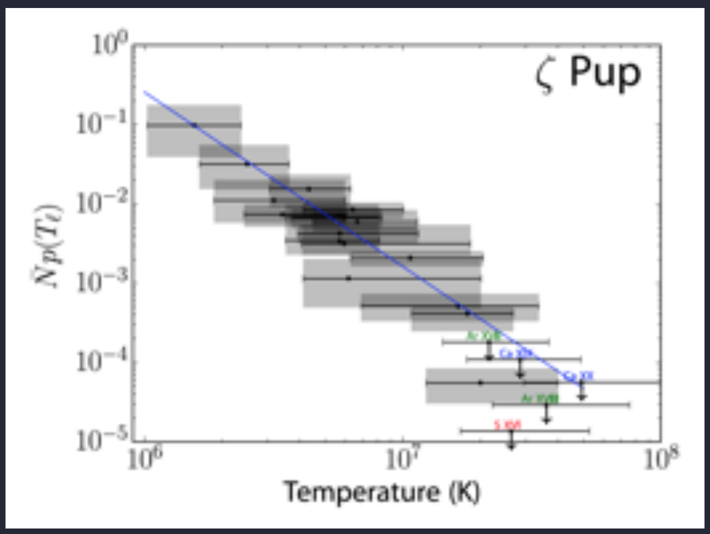

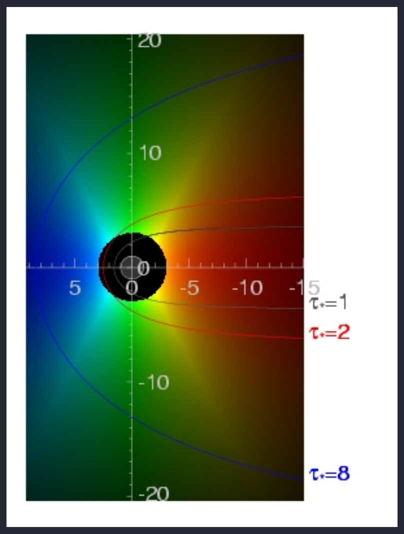

Soft-X-ray emission is ubiquitous in O stars

$L_X \sim 10^{-7} L_{Bol}$ ($L_X \sim 10^{31}$ to 10^{33} ergs s^{-1})

soft thermal spectrum: $kT < 1$ keV

minimal time variability

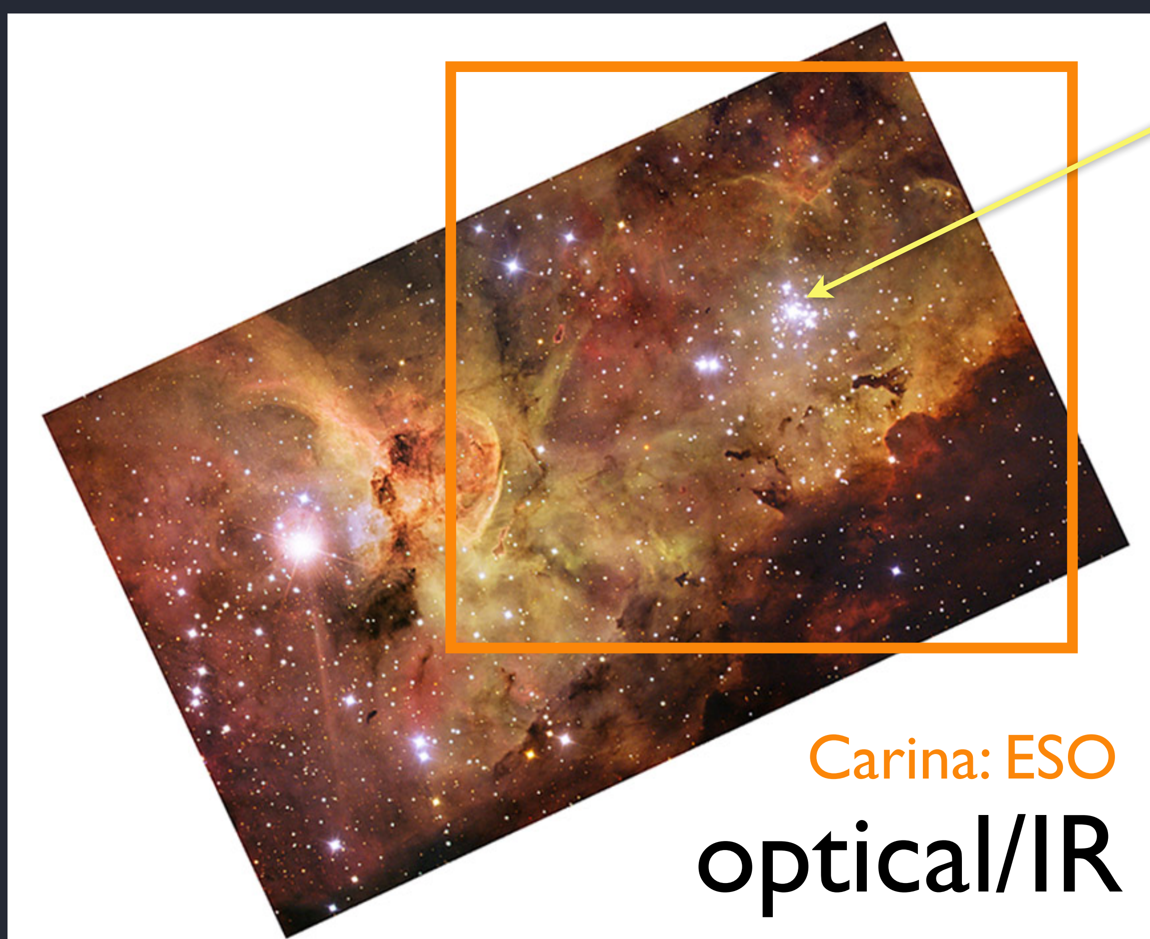

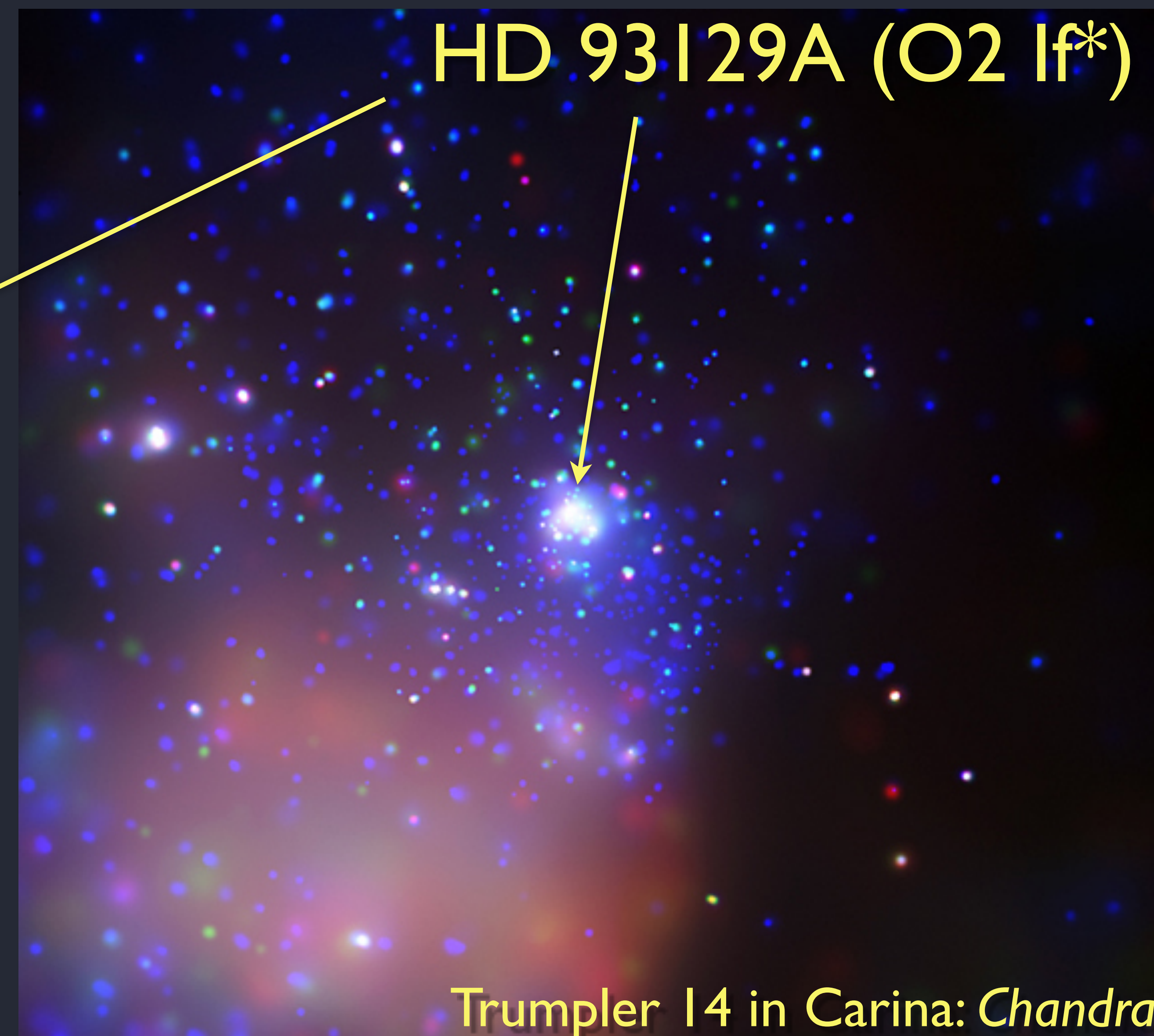

High- and low-mass stars have different X-ray production mechanisms

Massive stars show no correlation between rotation and X-ray emission
No convective envelope; no dynamo; no corona

X-ray luminosity

high mass

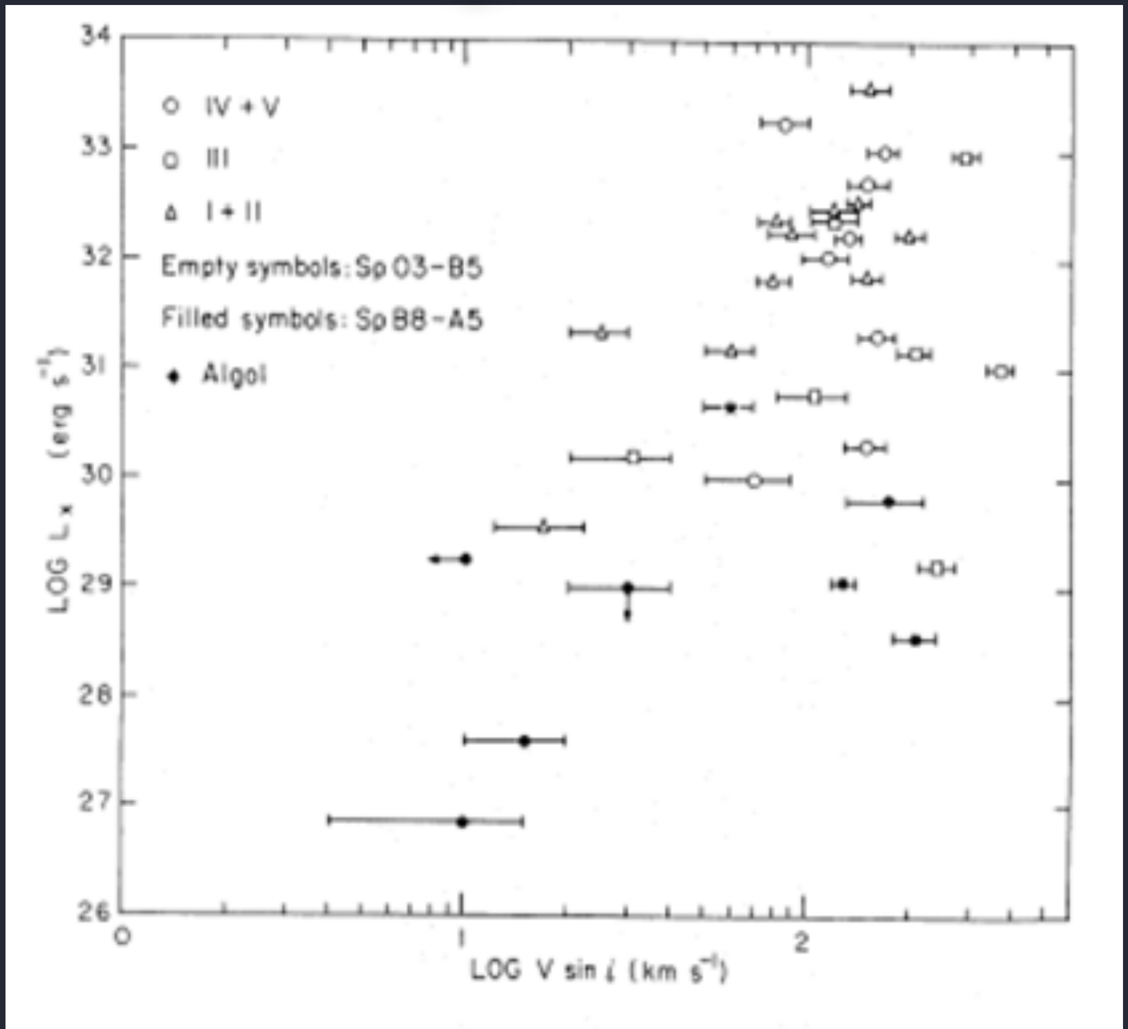

vsini

low mass

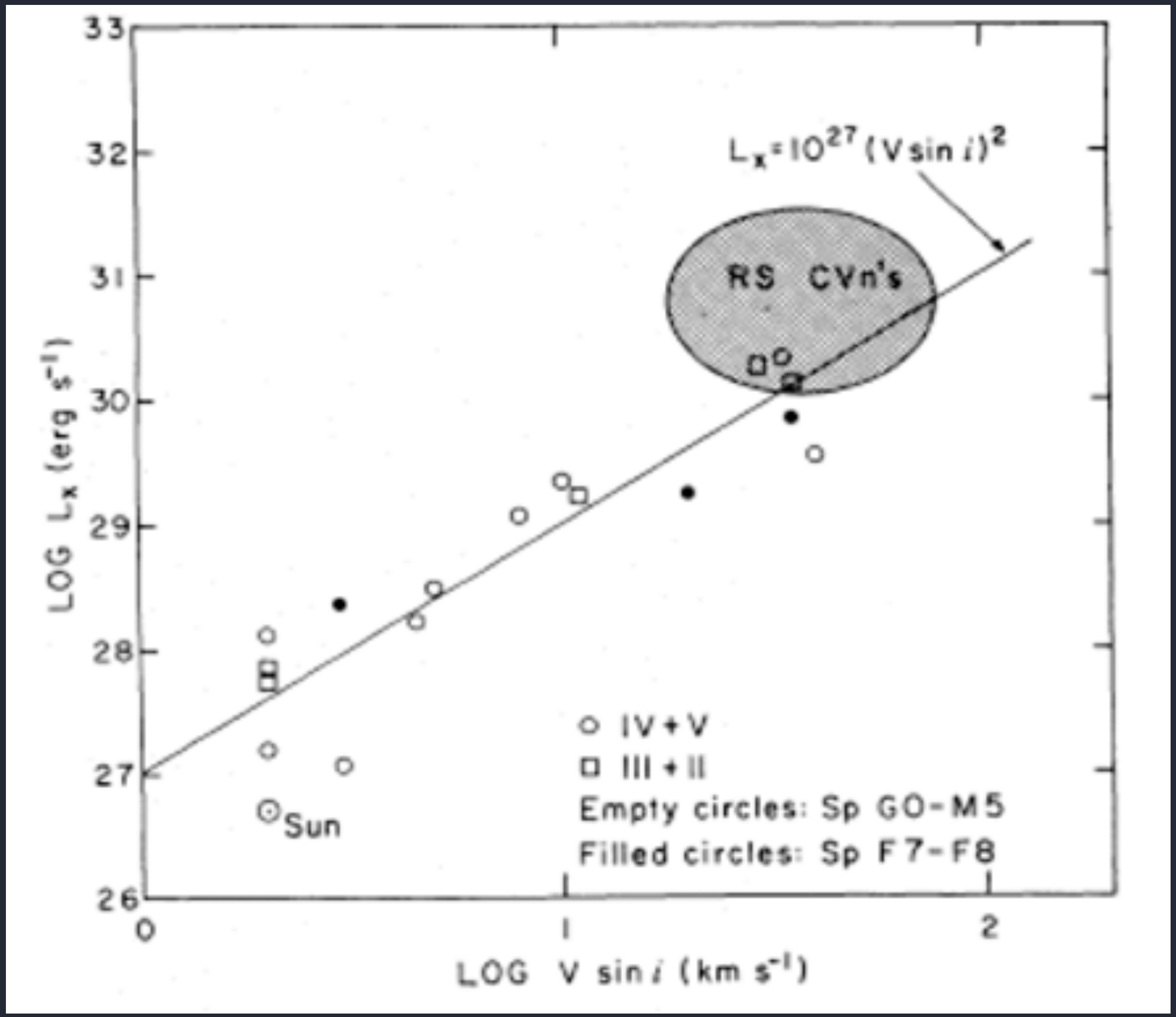

vsini

Radiation-driven O star winds

ζ Pup (O4 supergiant): $\dot{M} \sim$ few $10^{-6}\ M_{sun}/yr$

UV spectrum: C IV 1548, 1551 Å

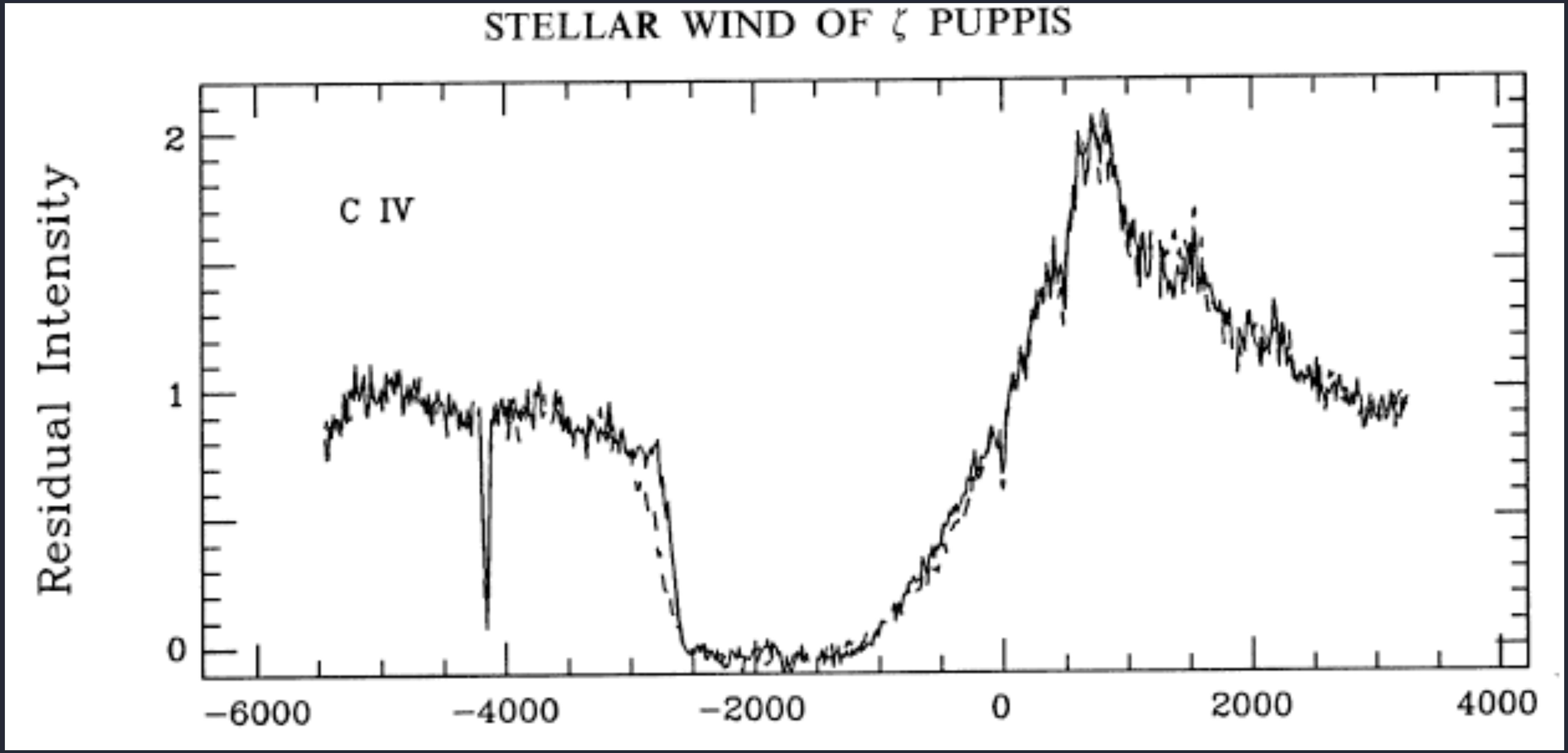

Velocity (km/s)

Prinja et al. 1992, ApJ, 390, 266

Chandra Medium Energy Grating (MEG)

ζ Pup (O4 If)

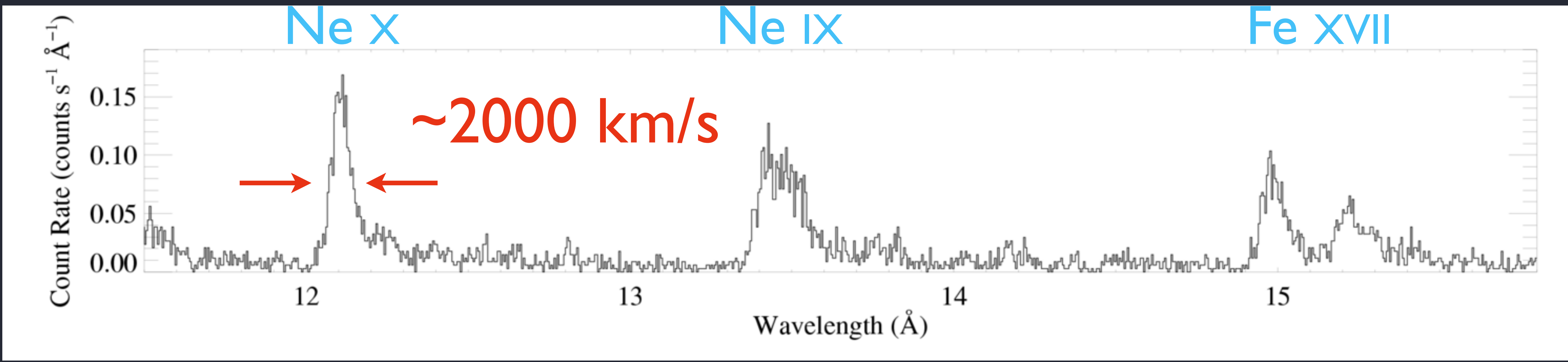

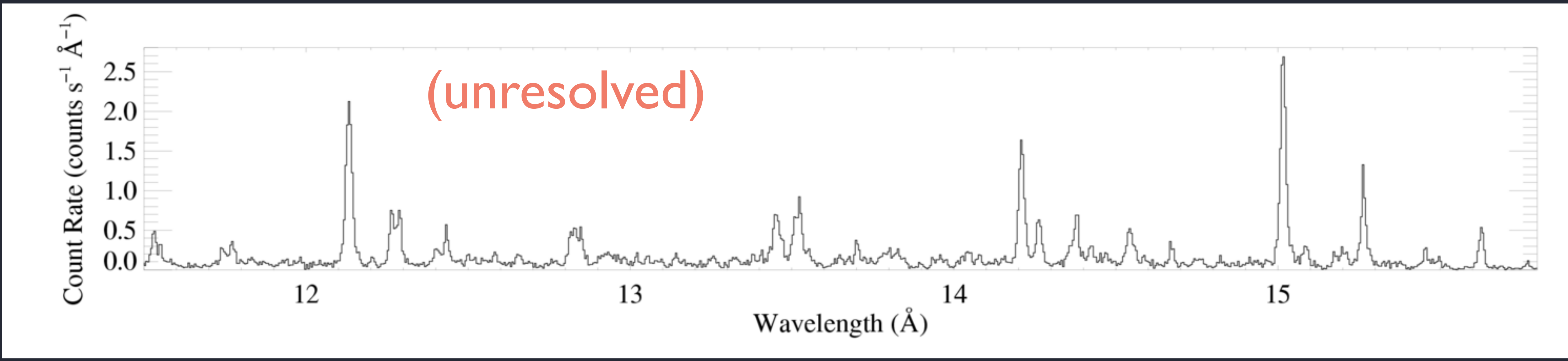

Capella (G5 III)

X-ray lines are Doppler-broadened => the X-ray emitting plasma is associated with the stellar wind

Radiation-driven O star winds

kinetic power in the wind = $1/2\ \dot{M} v_\infty^2$ ($\sim 10^{-3}\ L_{bol}$)

typically 10^4 times larger than the observed L_x

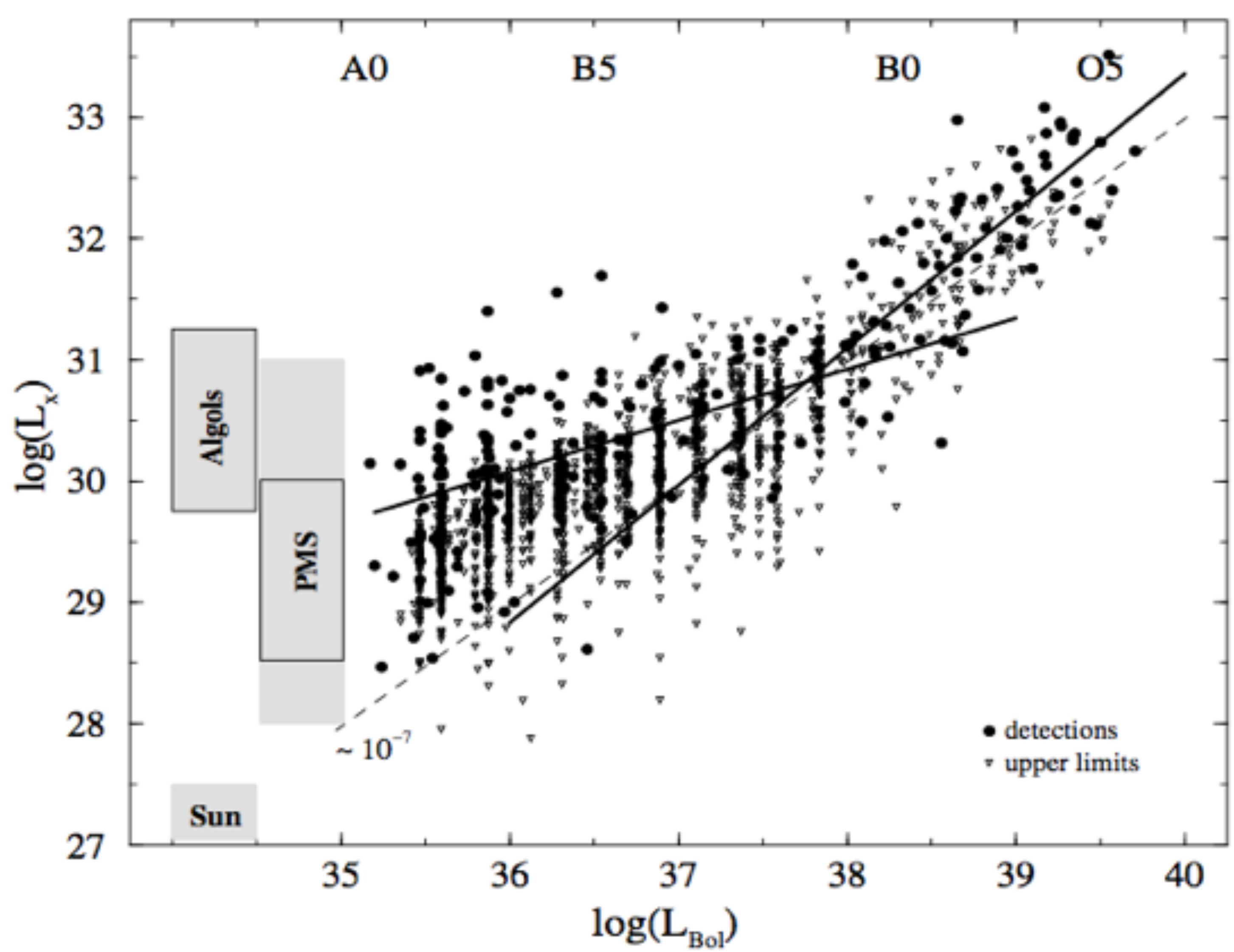

$L_x \sim 10^{-7}\ L_{bol}$

for O stars

Fig. 4. X-ray luminosities L_x plotted versus bolometric luminosities L_{Bol}; solid lines represent regression lines for $L_{Bol} < 10^{38} erg\ s^{-1}$ and $L_{Bol} > 10^{38}$ erg s^{-1}, whereas the dashed line shows $L_x = 10^{-7} \times L_{Bol}$, grey bars at the left side show typical ranges for the X-ray luminosity of Algol-type systems, pre-main sequence stars (PMS), and our Sun.

X-rays = thermal emission = ~10^{-4} of wind KE

…How is this small fraction of the wind kinetic energy extracted ?

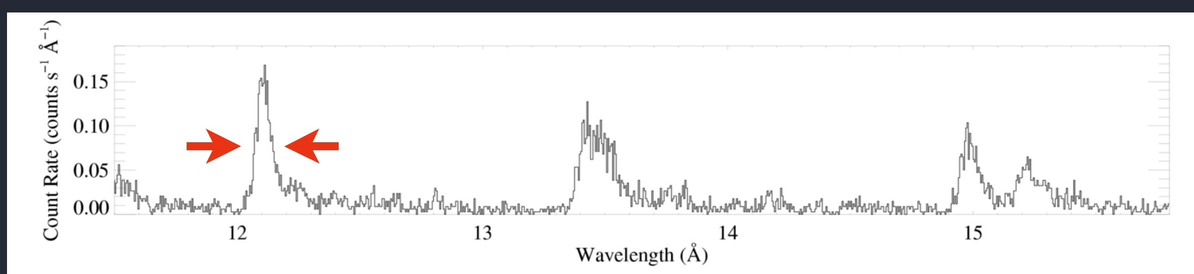

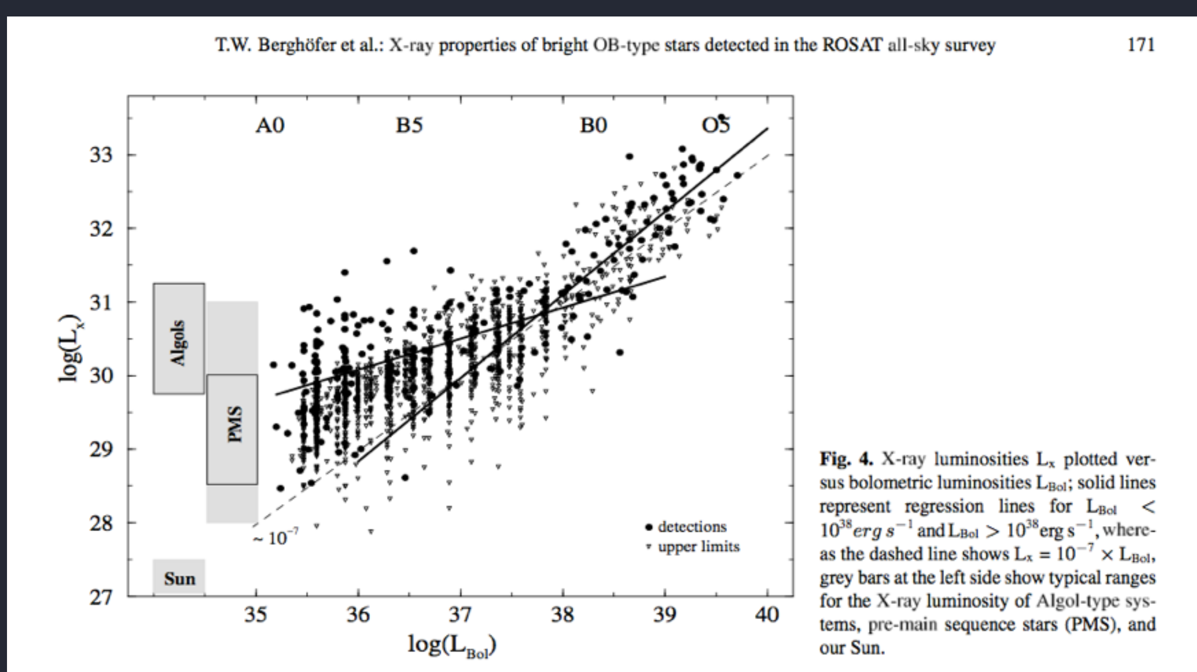
T.W. Berghöfer et al.: X-ray properties of bright OB-type stars detected in the ROSAT all-sky survey 171

Fig. 4. X-ray luminosities L_x plotted versus bolometric luminosities L_{Bol}; solid lines represent regression lines for $L_{Bol} < 10^{38} erg\,s^{-1}$ and $L_{Bol} > 10^{38}$ erg s^{-1}, whereas the dashed line shows $L_x = 10^{-7} \times L_{Bol}$, grey bars at the left side show typical ranges for the X-ray luminosity of Algol-type systems, pre-main sequence stars (PMS), and our Sun.

Embedded Wind Shock (EWS) paradigm

Line Deshadowing Instability (LDI) - intrinsic to line-driven flows

numerous shocks distributed throughout the wind, generally above some onset radius

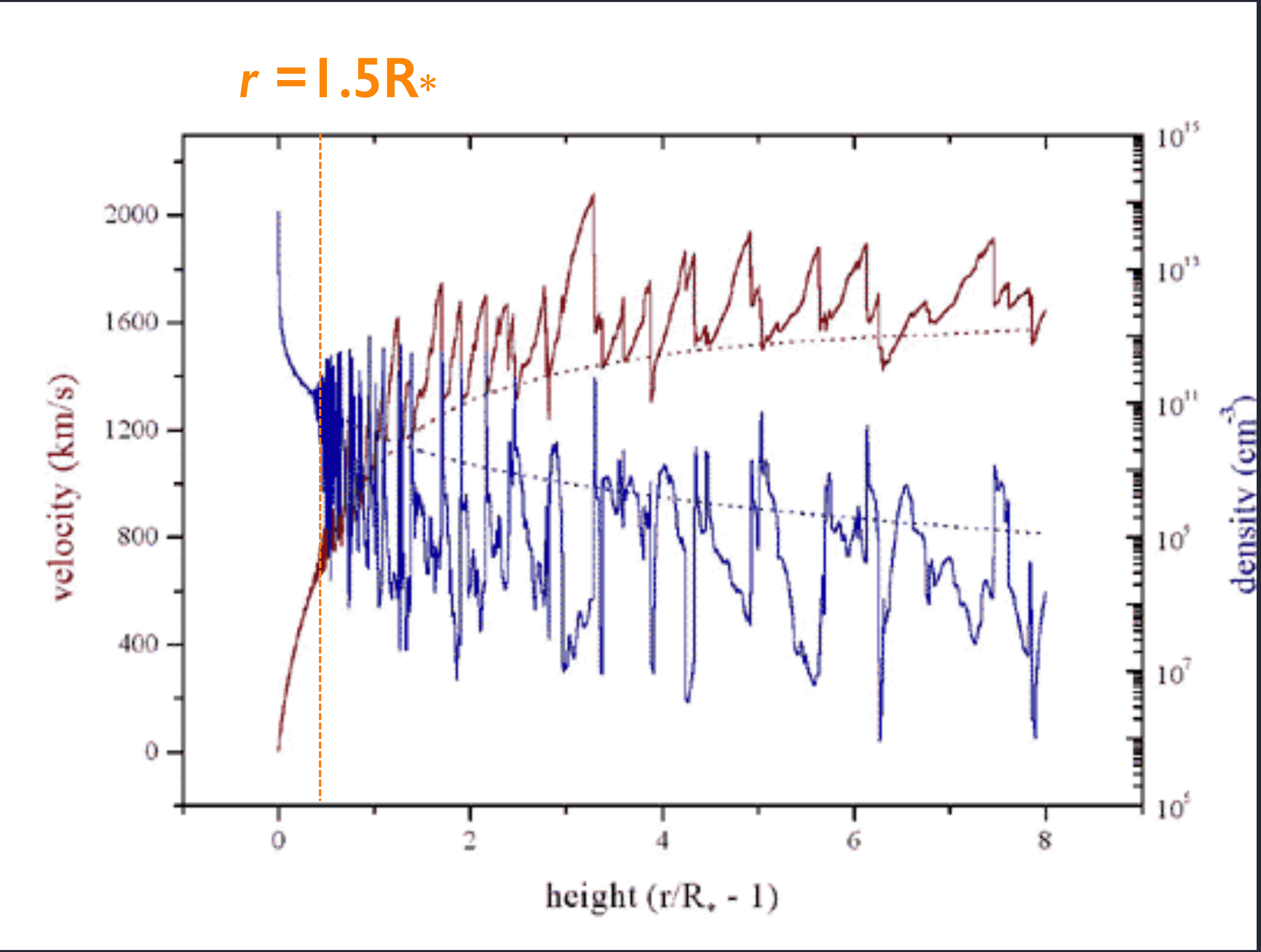

1-D radiation-hydro simulation

Embedded Wind Shock (EWS) paradigm

Less than 1% of the mass of the wind is emitting X-rays

>99% of the wind is cold and X-ray *absorbing*

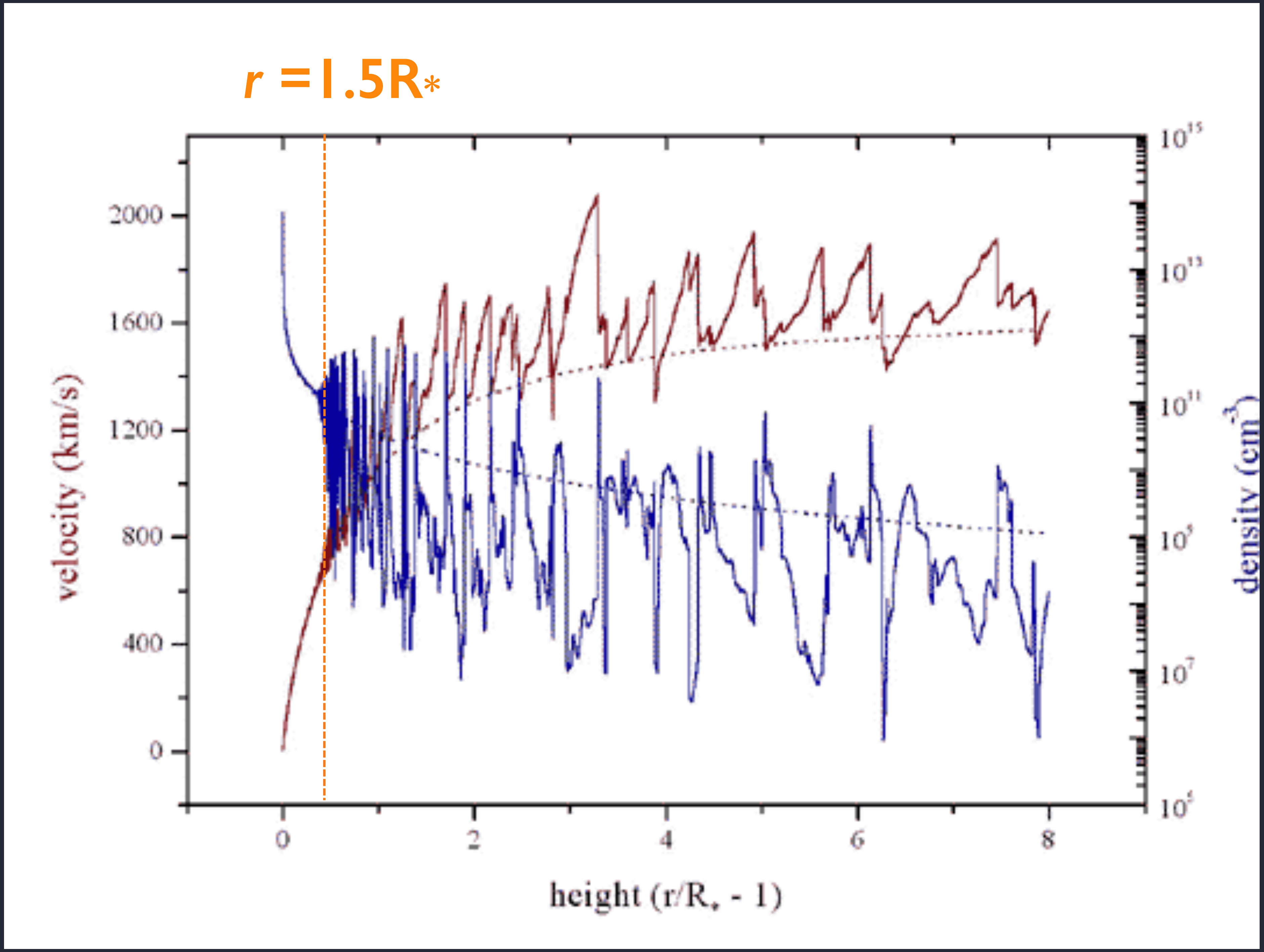

1-D rad-hydro simulation

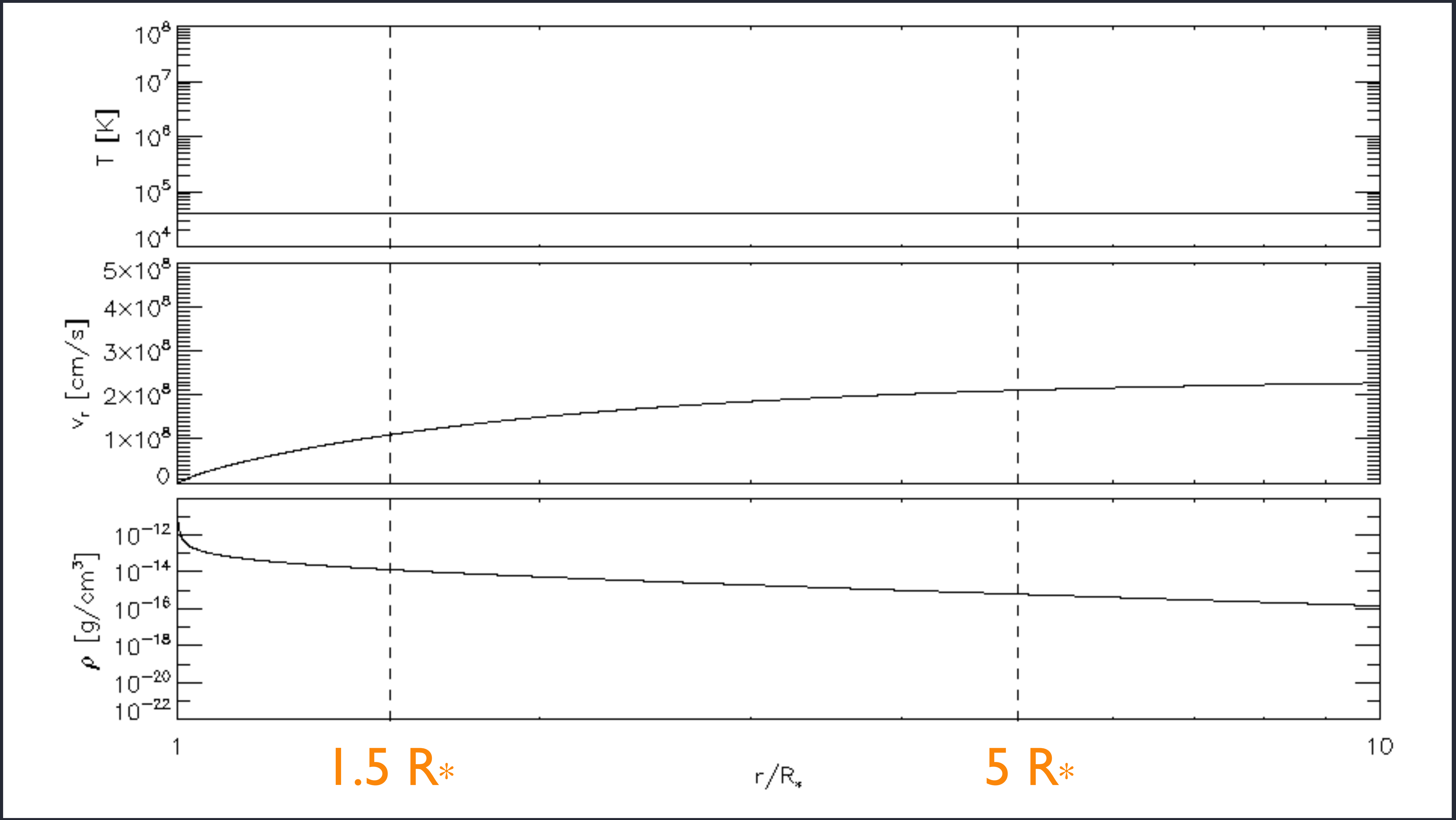

with J. Sundqvist, S. Owocki, Z. Li

An animated gif of this simulation is available at
http://astro.swarthmore.edu/~cohen/presentations/JOS_sim_lowkappamax.gif

2-D radiation-hydro simulations

initial work 12 years ago; line transport is expensive

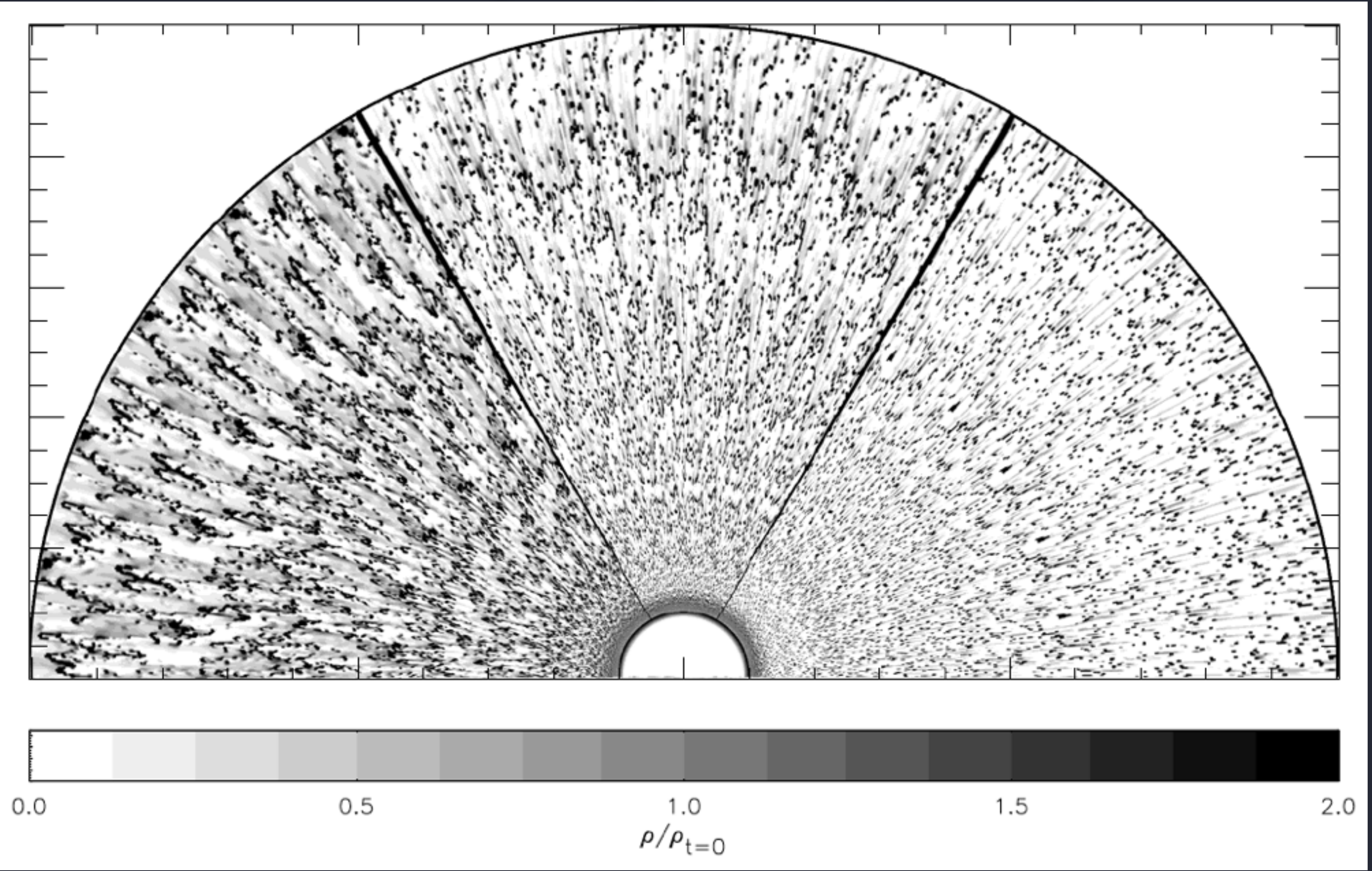

Dessart & Owocki 2003

Line-Deshadowing Instability (LDI)

LDI (Milne 1926) is intrinsic to any radiation-driven outflow in which the momentum transfer is mediated by spectral lines

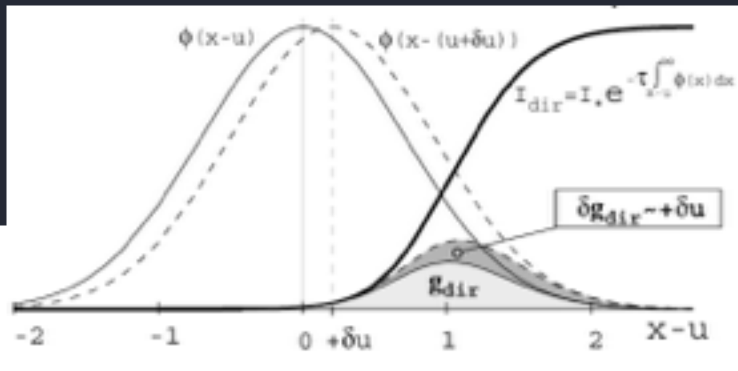

rapidly accelerating material moves out of the Doppler shadow of the material behind it

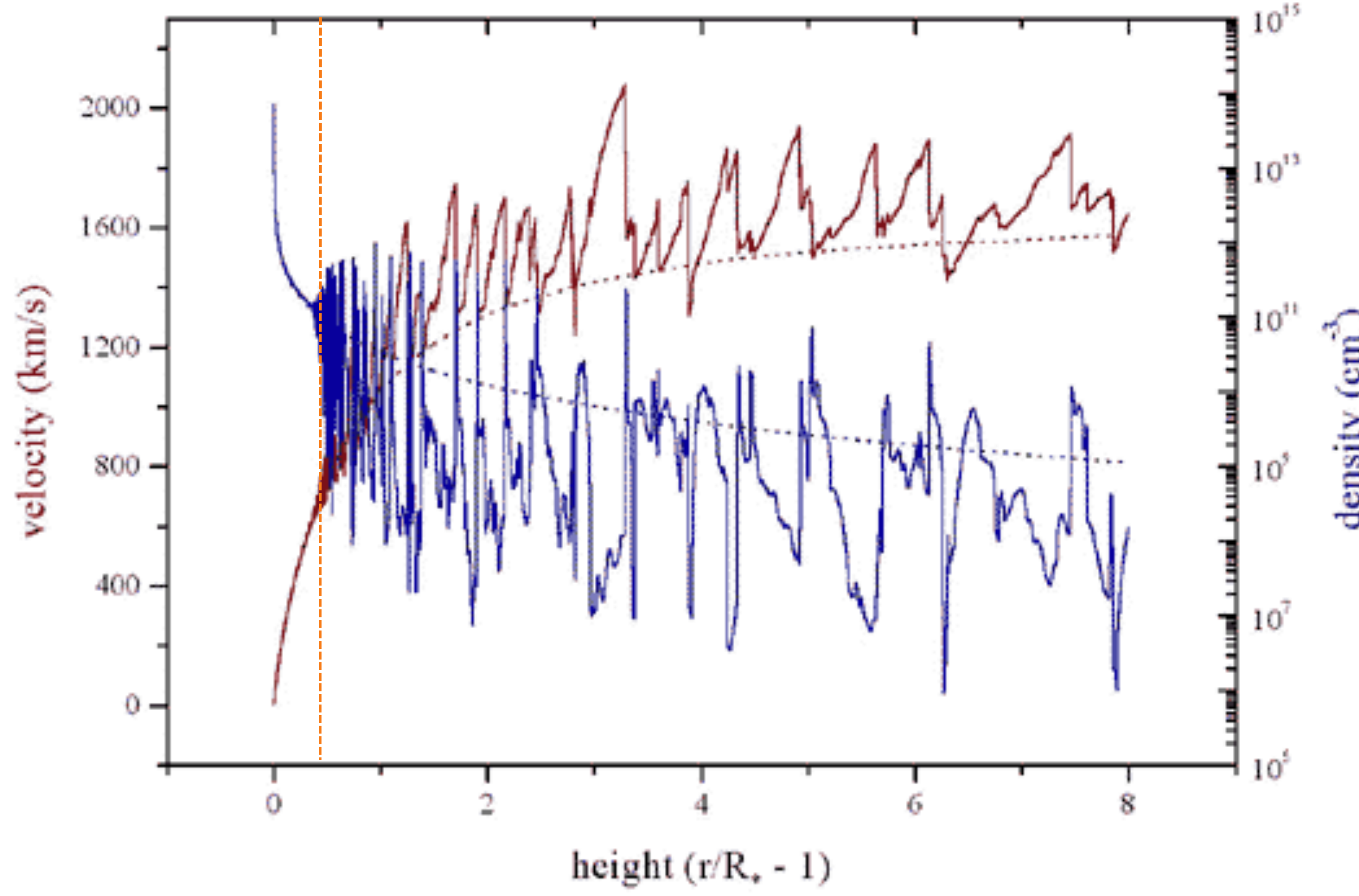

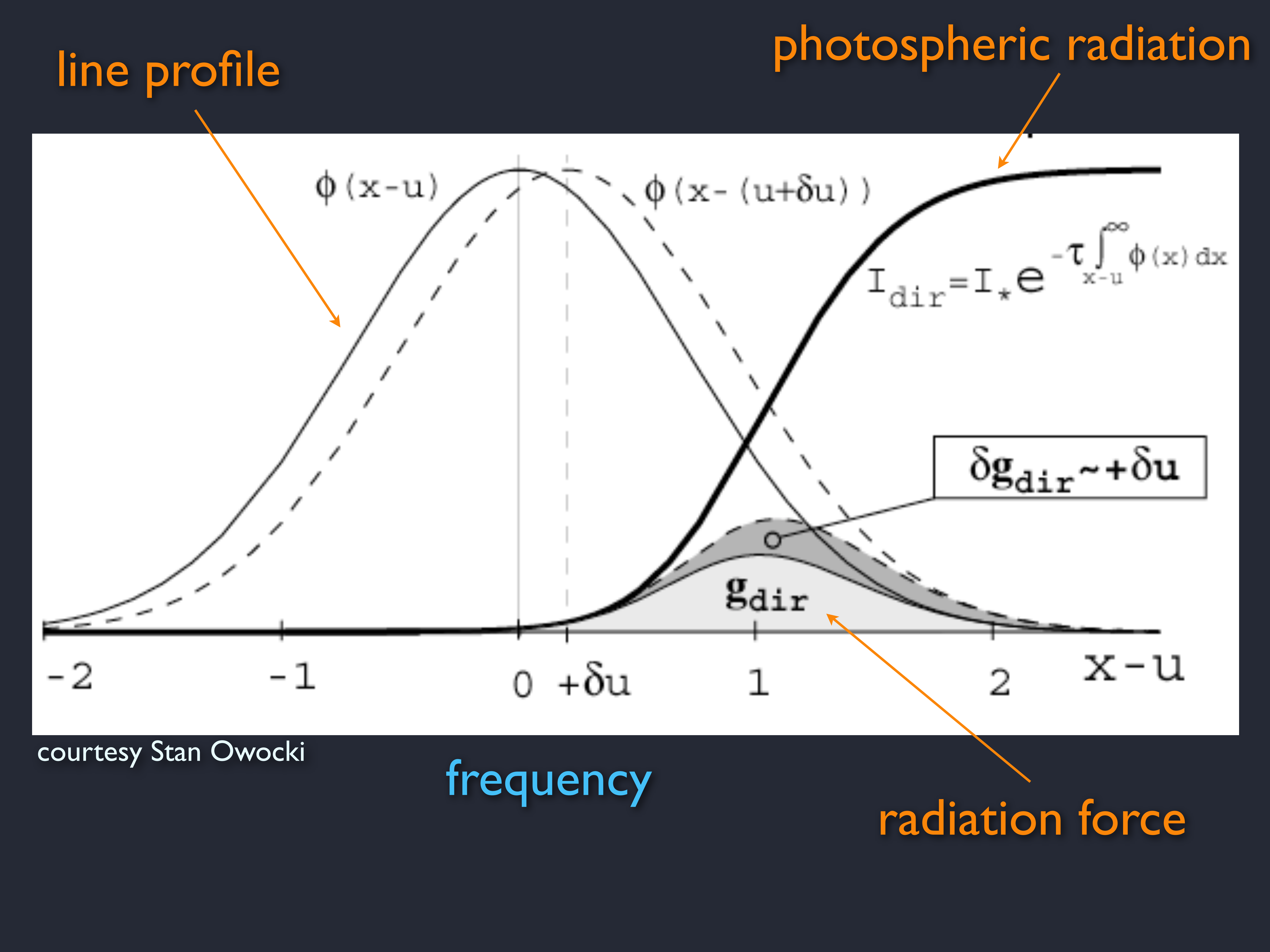
line profile
photospheric radiation
ϕ(x-u)
ϕ(x-(u+δu))
$I_{dir}=I_* e^{-\tau \int_{x-u}^{\infty} \phi(x)\,dx}$
$\delta g_{dir} \sim +\delta u$
g_{dir}
-2
-1
0
+δu
1
2
x-u
courtesy Stan Owocki
frequency
radiation force

line profile

the Doppler shadow

photospheric radiation

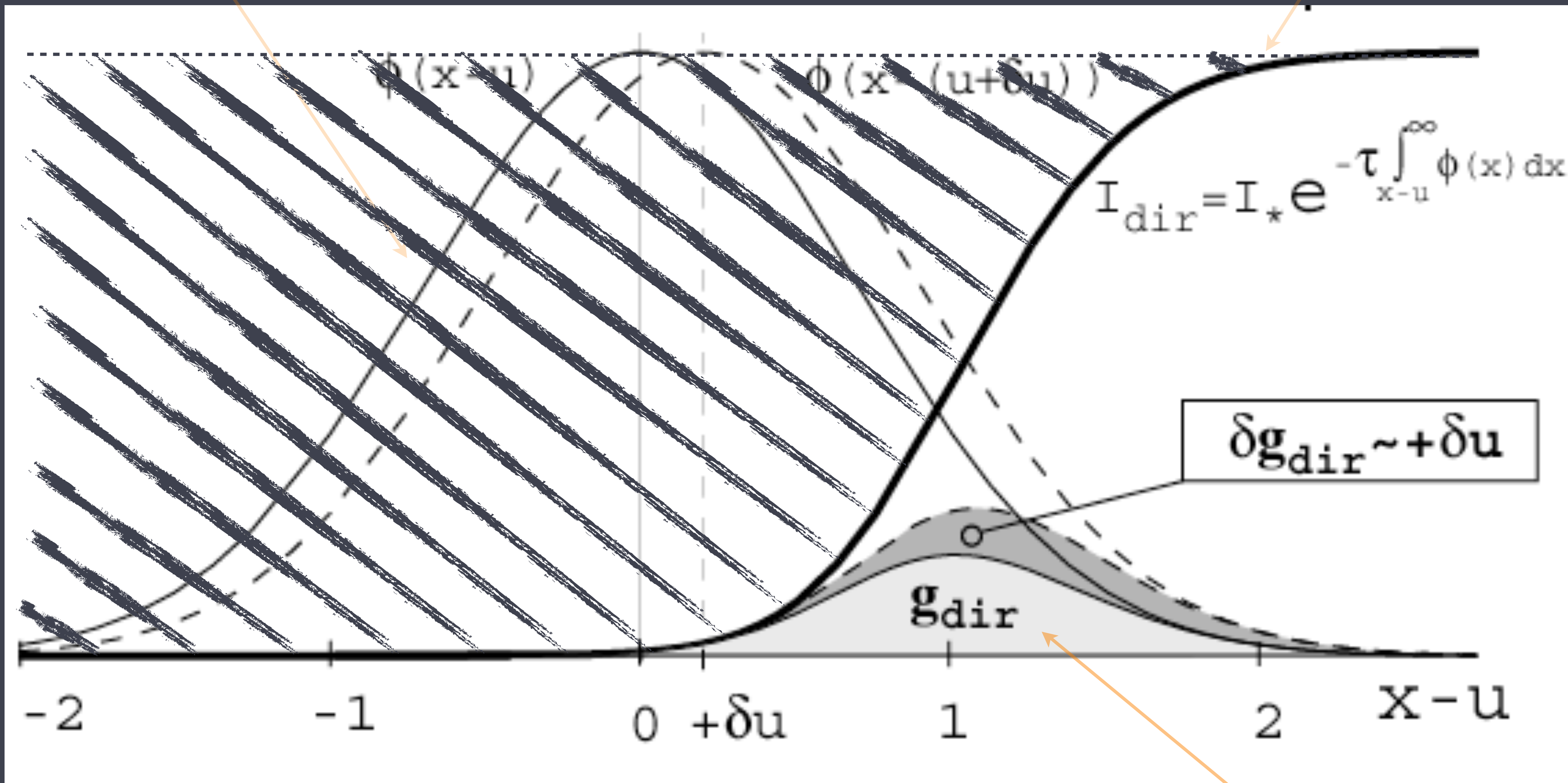

frequency

radiation force

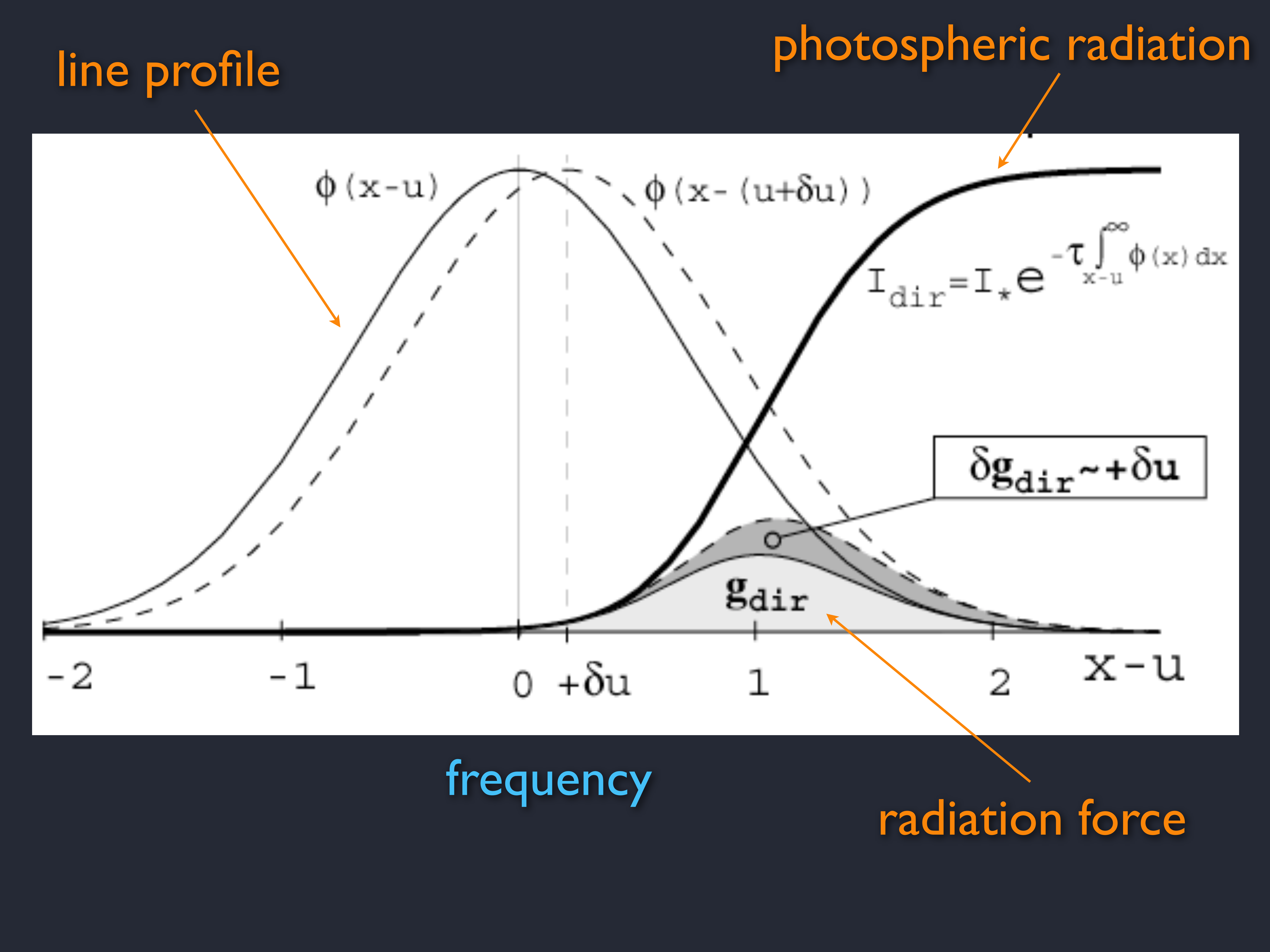
line profile
photospheric radiation
φ (x-u)
φ (x- (u+δu))
$I_{dir}=I_{*}e^{-\tau\int_{x-u}^{\infty}\phi(x)\,dx}$
$\delta g_{dir}\sim+\delta u$
g_{dir}
-2
-1
0
+δu
1
2
x-u
frequency
radiation force

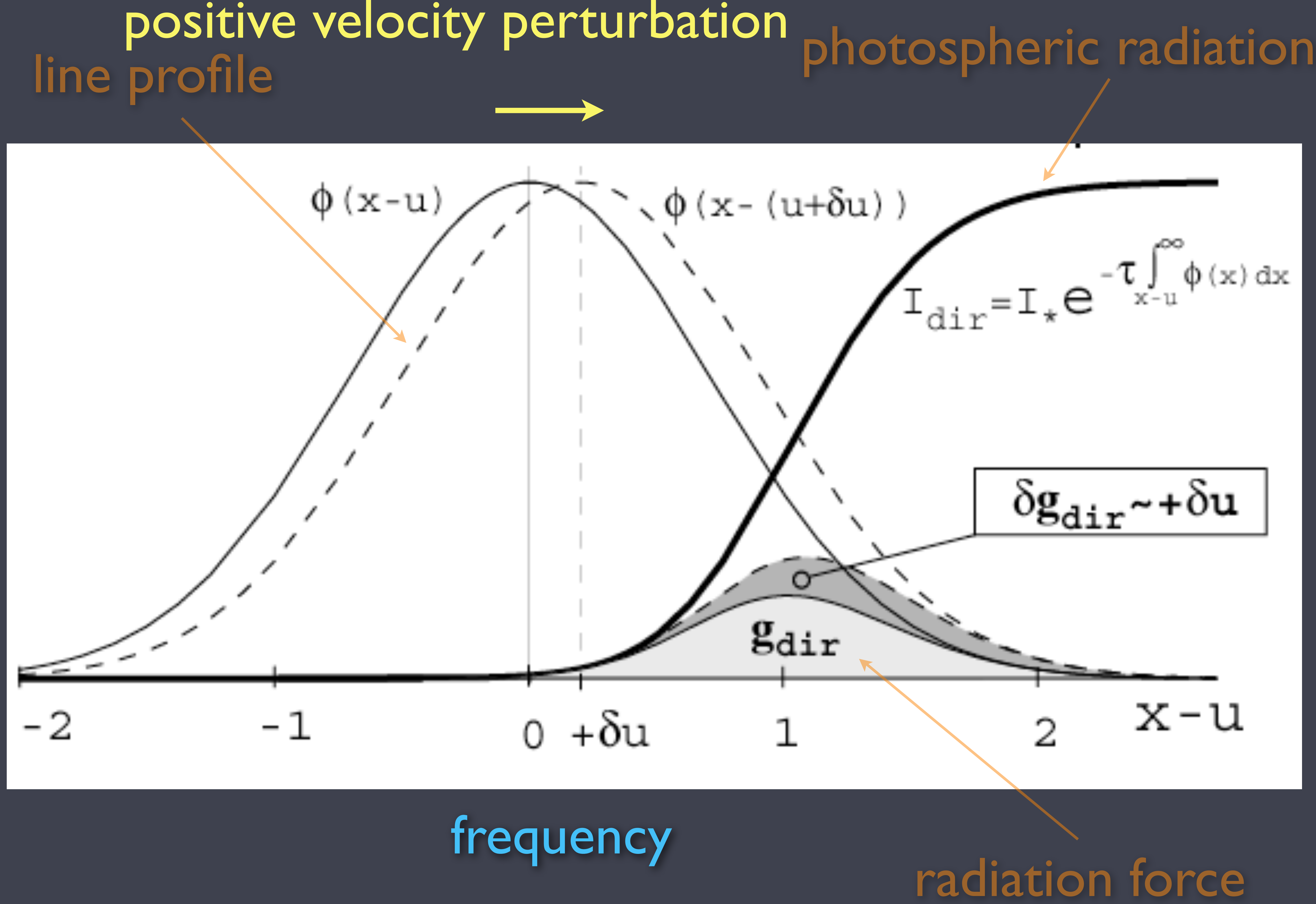

positive velocity perturbation
line profile
photospheric radiation
ϕ (x-u)
ϕ (x- (u+δu))
$I_{dir}=I_* e^{-\tau \int_{x-u}^{\infty} \phi(x)\,dx}$
$\delta g_{dir} \sim +\delta u$
g_{dir}
-2
-1
0
+δu
1
2
x-u
frequency
radiation force

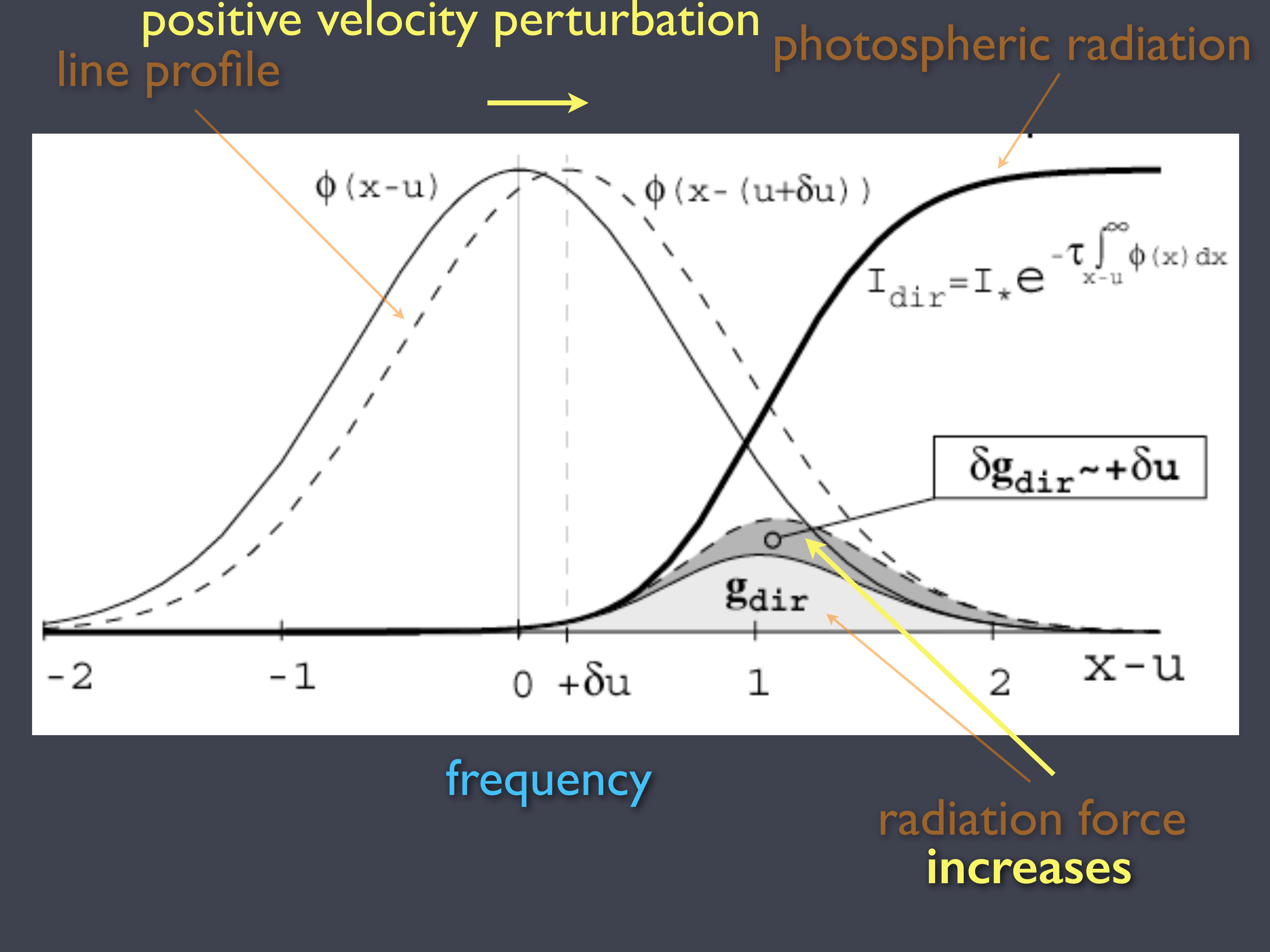
positive velocity perturbation
line profile
photospheric radiation
ϕ (x-u)
ϕ (x- (u+δu))
$I_{dir}=I_* e^{-\tau \int_{x-u}^{\infty} \phi(x)\,dx}$
$\delta g_{dir} \sim +\delta u$
g_{dir}
-2
-1
0
+δu
1
2
x-u
frequency
radiation force
increases

Physics of the Line Deshadowing Instability (LDI)

radiation force depends on changes in the local wind velocity (moving out of the Doppler shadow), but acceleration depends on the force (Newton): strong feedback and resulting instability

stability analysis: Owocki, Castor, Rybicki (1988)

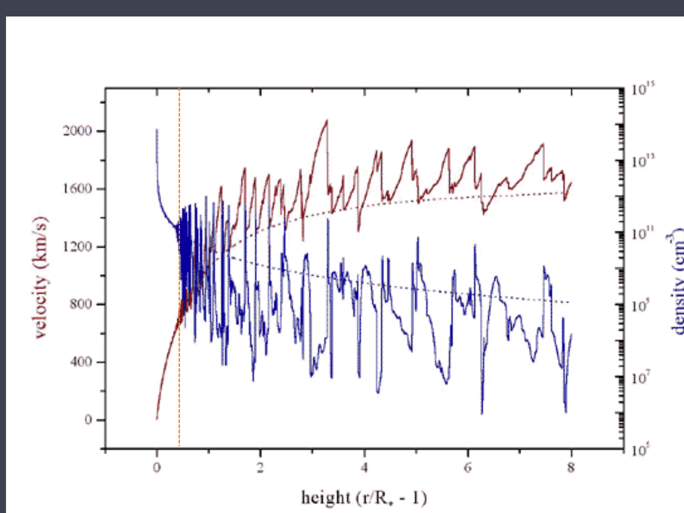

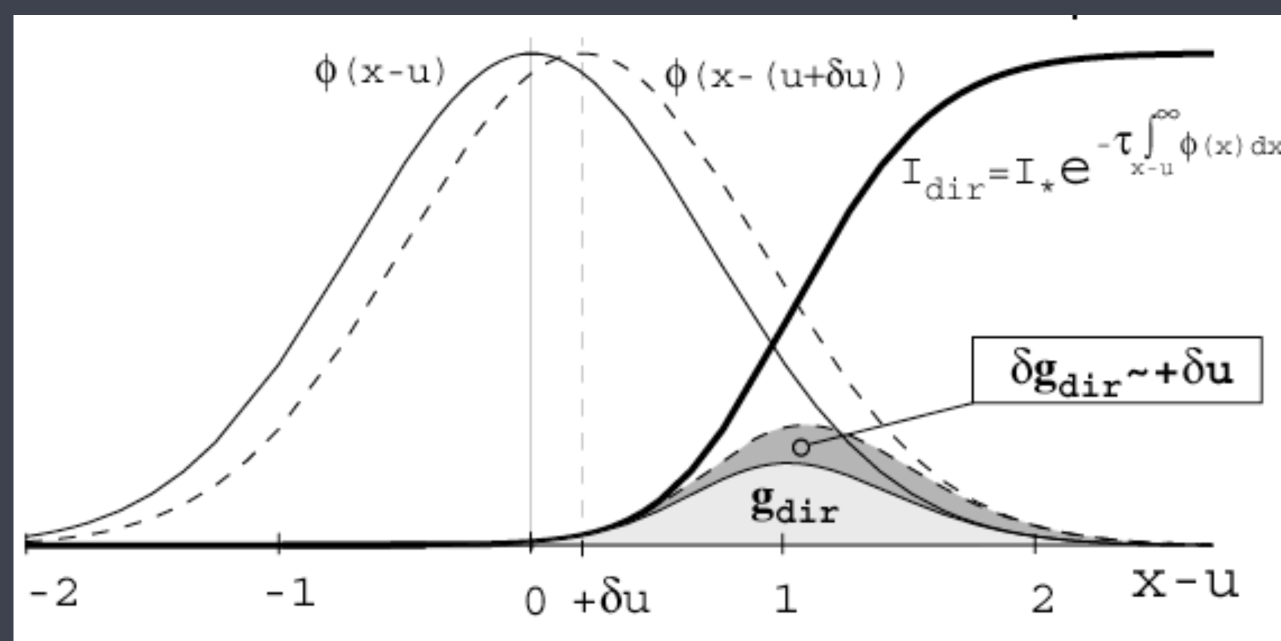

put detailed spectral line transport in a radiation-hydro code

2.1. Conservation equations

Consider an inviscid flow along the radial direction r from a central star. In Eulerian form, the one-dimensional (1D) time-dependent equations for conservation of mass, momentum, and energy are:

$$\frac{\partial \rho}{\partial t} + \frac{1}{r^2}\frac{\partial (r^2 \rho v)}{\partial r} = 0 \quad (1)$$

$$\frac{\partial (\rho v)}{\partial t} + \frac{1}{r^2}\frac{\partial (r^2 \rho v^2)}{\partial r} = -\frac{\partial p}{\partial r} - \rho g_* + \rho g_{\rm rad} \quad (2)$$

$$\frac{\partial e}{\partial t} + \frac{1}{r^2}\frac{\partial (r^2 e v)}{\partial r} = -\frac{p}{r^2}\frac{\partial (r^2 v)}{\partial r} - Q_{\rm rad}. \quad (3)$$

Feldmeier, Puls, & Pauldrach (1997)

Simulations constrained by data?

Can we reliably compute an X-ray spectrum from the simulations to compare to observations?

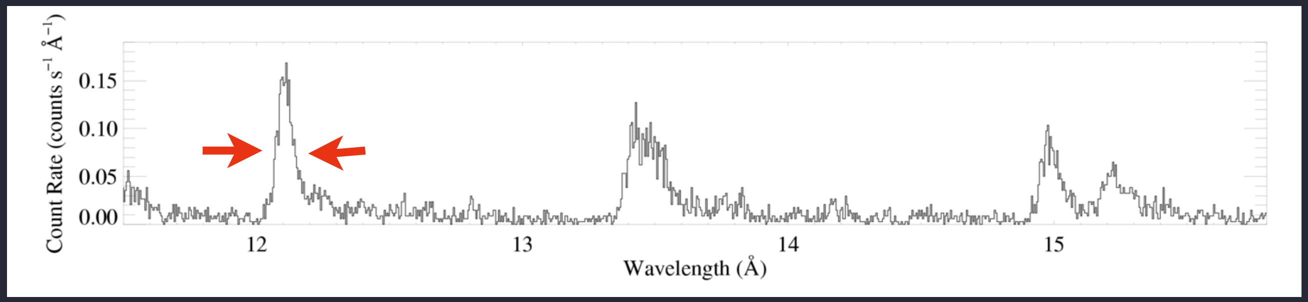

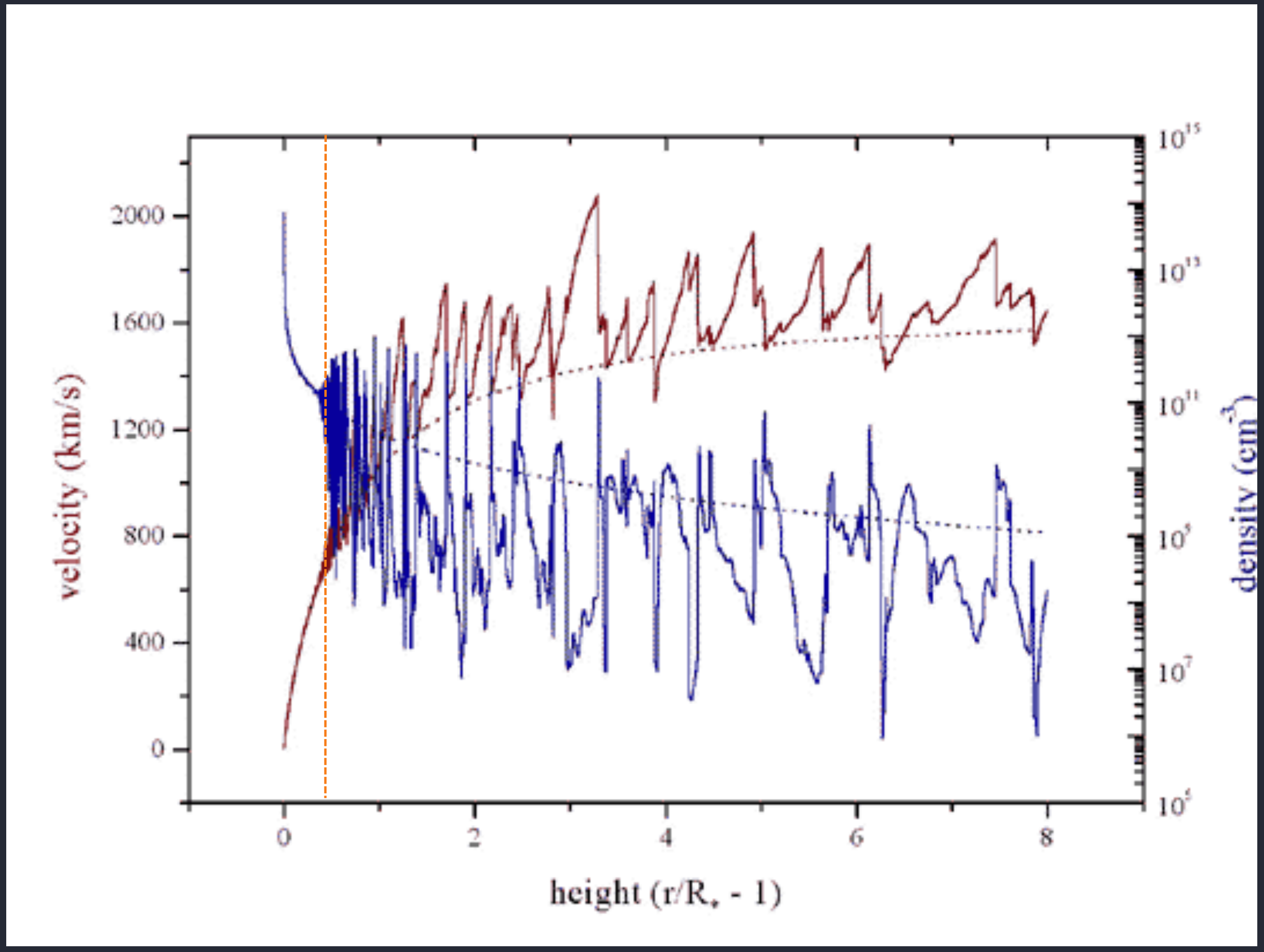

No. Not easily, anyway.

Resolving post-shock gas as it advects across the grid is very difficult.

Numerical instabilities related to radiative cooling are difficult to combat.

Several additional computational and physics issues: 1-D limitation; line-force cut-off; lower boundary conditions (to be discussed at the end).

Open Questions

How efficient is the LDI at making shocks? How many shocks?

What is the distribution of shock strengths (temperatures)?

What is the spatial distribution of shocks?

How clumped is the wind?

Big Question

what are the actual mass-loss rates of O star winds?

Key issues addressed by new work

How efficient is the LDI at making shocks? How many shocks?

What is the distribution of shock strengths (temperatures)?

What is the spatial distribution of shocks?

How clumped is the wind?

Key issues addressed by new work

What is the distribution of shock strengths (temperatures)?

closely related to: "what is the instantaneous distribution of plasma temperatures?" (the differential emission measure)

but this involves *cooling* as well as heating

And the cooling is difficult to model in detail in the numerical simulations

Traditional emission measure approach

coronal (thermal, equilibrium, collisional, optically thin) X-ray emission scales as density *squared*

$$EM = \int \rho^2 dVol$$

$$L_x = EM \times \Lambda(T, \lambda)$$

emission measure (EM) is a function of temperature

$$L_x = \int \frac{dEM}{dT} \Lambda(T, \lambda) dT$$

differential emission measure (DEM)

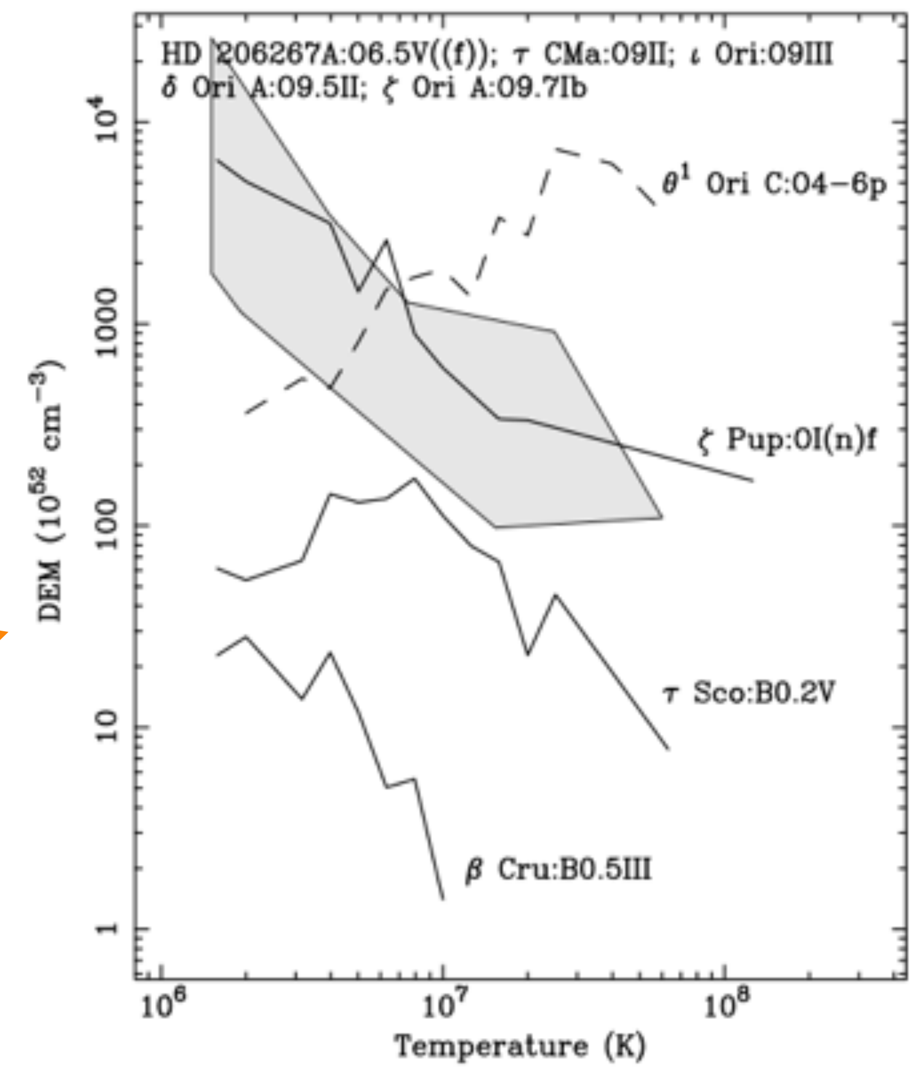

Fig. 5.—Composite approximate representation of the DEM constraints we derive for the nine stars. The filled polygon encloses the lines for HD 206267A, ι Ori, ζ Pup, ζ Ori A, τ CMa, and δ Ori A, which are very similar and difficult to show together. The jagged shape of the curves gives some idea of the magnitude of the error for the DEM constraints. Details of the construction of this figure are given in the text.

Wojdowski & Schulz (2005)

Problems with the (D)EM

depends on the density (squared) of the hot plasma

overall level doesn’t tell you about the efficiency or rate of the heating…without a lot of modeling

temperature distribution depends on the cooling as well as the heating

A new method for directly extracting information about shock heating from an X-ray spectrum

Monthly Notices of the ROYAL ASTRONOMICAL SOCIETY

MNRAS **444,** 3729–3737 (2014) doi:10.1093/mnras/stu1661

Measuring the shock-heating rate in the winds of O stars using X-ray line spectra

David H. Cohen,[1★] Zequn Li,[1] Kenneth G. Gayley,[2] Stanley P. Owocki,[3] Jon O. Sundqvist,[3,4] Véronique Petit[3,5] and Maurice A. Leutenegger[6,7]

[1] *Swarthmore College, Department of Physics and Astronomy, Swarthmore, PA 19081, USA*
[2] *University of Iowa, Department of Physics and Astronomy, Iowa City, IA 52242, USA*
[3] *University of Delaware, Bartol Research Institute, Newark, DE 19716, USA*
[4] *Institut für Astronomie und Astrophysik der Universität München, Scheinerstr. 1, D-81679 München, Germany*
[5] *Florida Institute of Technology, Department of Physics and Space Sciences, Melbourne, FL 32901, USA*
[6] *NASA/Goddard Space Flight Center, Code 662, Greenbelt, MD 20771, USA*
[7] *CRESST and University of Maryland, Baltimore County, Baltimore, MD 21250, USA*

The method is surprisingly simple, because O star wind shocks are radiative. But the framework developed by Gayley (2014) can incorporate other cooling channels (adiabatic, conduction)

Dense O star winds have radiative shocks

the X-ray emission level scales *not* as density squared but linearly with density

L_x from one shock-heated particle, integrated over its cooling ~ kT_{shock}

Total L_x from a shock ~ mass flux across the shock front (times the kT_{shock} for each particle)

there is a large, statistical sample of shocks representing all stages of shock evolution - a single X-ray observation is equivalent to completely tracking the evolution of a representative ensemble of shocks.

Dense O star winds have radiative shocks

insight (e.g. Antokhin et al. 2004; Gayley 2014):

if radiation is the dominant cooling mechanism, the time-integrated spectrum of the post-shock plasma as it cools only depends on the initial shock temperature

not on the density; higher density cools faster but emits more strongly

THE ASTROPHYSICAL JOURNAL

The Astrophysical Journal > Volume 788 > Number 1

Thermal X-Ray Spectral Tools. I. Parameterizing Impulsive X-Ray Heating with a Cumulative Initial Temperature (CIT) Distribution

Kenneth G. Gayley
Show affiliations

Kenneth G. Gayley 2014 *ApJ* **788** 90. doi:10.1088/0004-637X/788/1/90
Received 26 January 2014, accepted for publication 15 April 2014. Published 27 May 2014.

Dense O star winds have radiative shocks

insight (e.g. Antokhin et al. 2004; Gayley 2014):

each X-ray emission line is sensitive to shocks corresponding to a given temperature, T_{line} - and so it radiates in plasma shock-heated to temperatures T_{line} *and greater*

Ne X: T_{line} = 6 X 10^6 K

ζ Pup (O4 If)

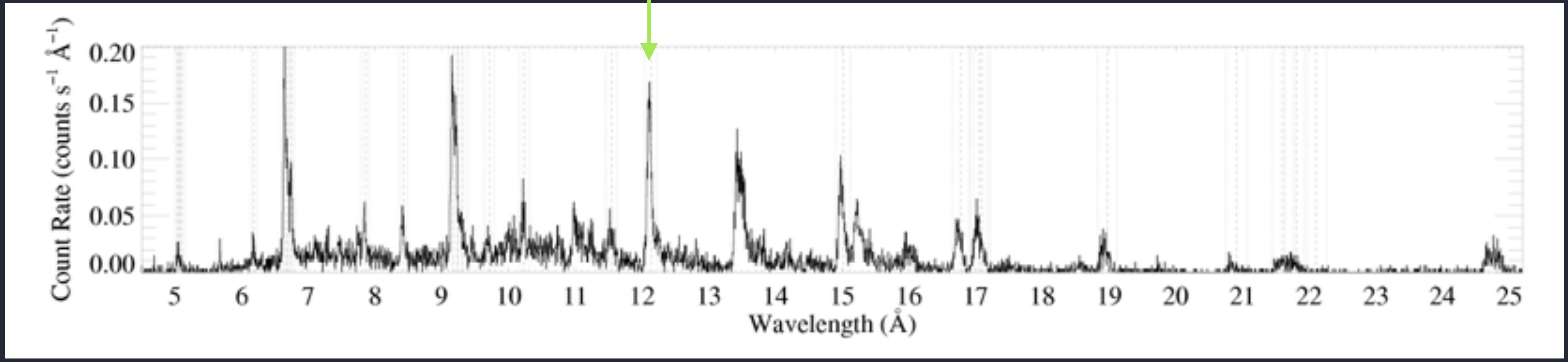

Dense O star winds have radiative shocks

The X-ray spectrum thus contains information - almost directly - about the *cumulative* probability distribution of shock strengths, $p(T)$ = the probability that a shock heats gas to at least T.

Ne X: $T_{line} = 6 \times 10^6$ K

ζ Pup (O4 If)

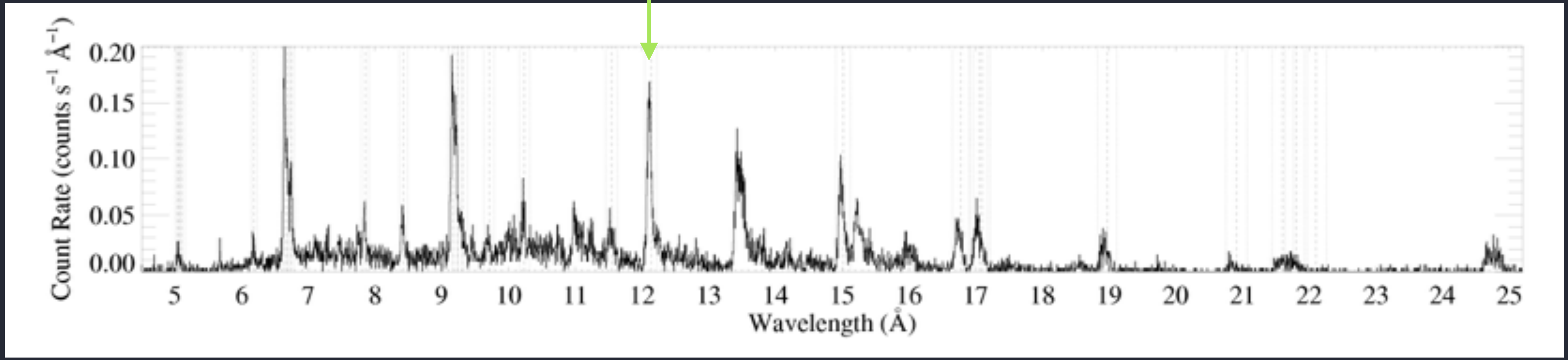

X-ray luminosity from shock properties

L_x from from a single shock, heated to temperature T_{shock}:

$$L_x = \frac{\dot{M}}{\mu m_p} k T_{shock} \bar{N}$$

$\bar{N}$, average number of times a particle crosses a shock front as it advects out through the wind

X-ray luminosity from shock properties

L_{line} X-ray luminosity radiated into a *single line* as a shock cools:

$$L_\ell = \frac{\dot{M}}{\mu m_p} \frac{5}{2} k \Delta T_\ell \bar{N}$$

fraction of shock energy radiated in the line

$\bar{N}$, average number of times a particle crosses a shock front as it advects out through the wind

$$\Delta T_\ell \equiv \int_0^\infty \frac{\Lambda_\ell(T)}{\Lambda(T)} \, \mathrm{d}T$$

(ignoring momentarily that not every shock is hot enough to generate emission in a given line)

emissivities from *APEC*

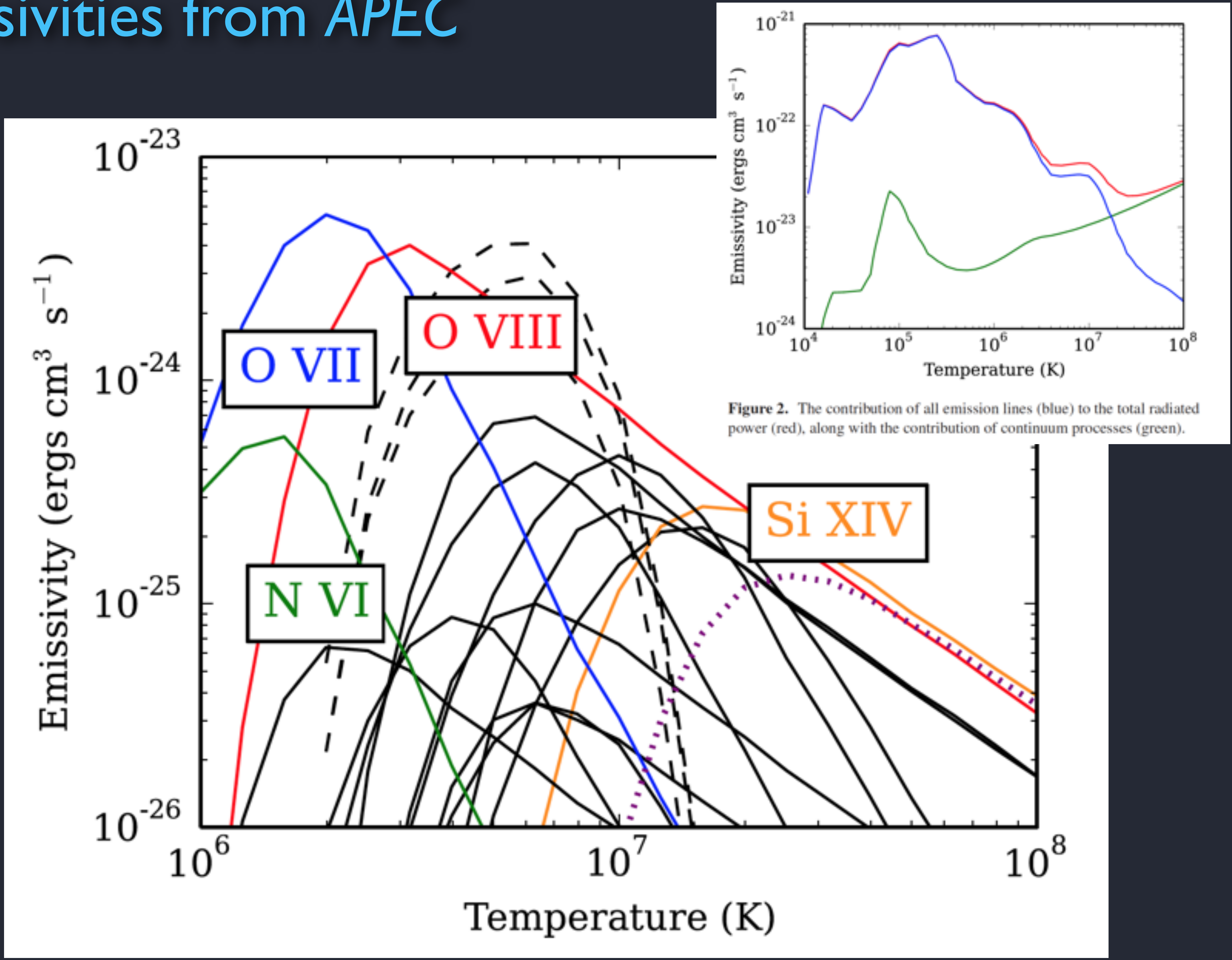

Figure 2. The contribution of all emission lines (blue) to the total radiated power (red), along with the contribution of continuum processes (green).

Smith et al. (2001); Foster et al. (2012)

fraction of shock energy radiated in the line

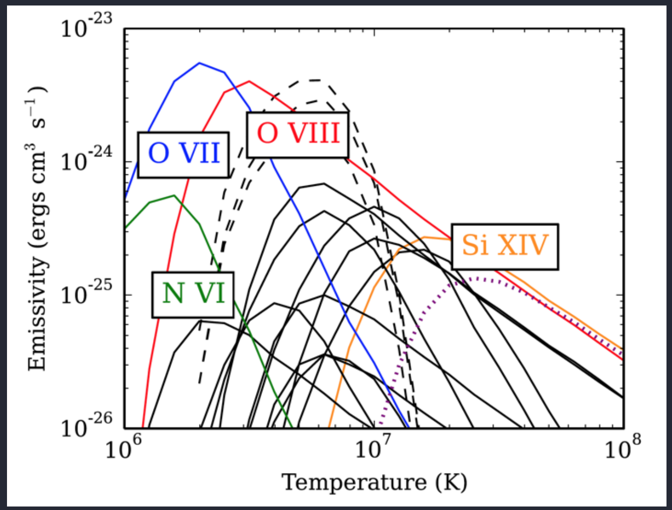

$$\Delta T_\ell \equiv \int_0^\infty \frac{\Lambda_\ell(T)}{\Lambda(T)}\, \mathrm{d}T$$

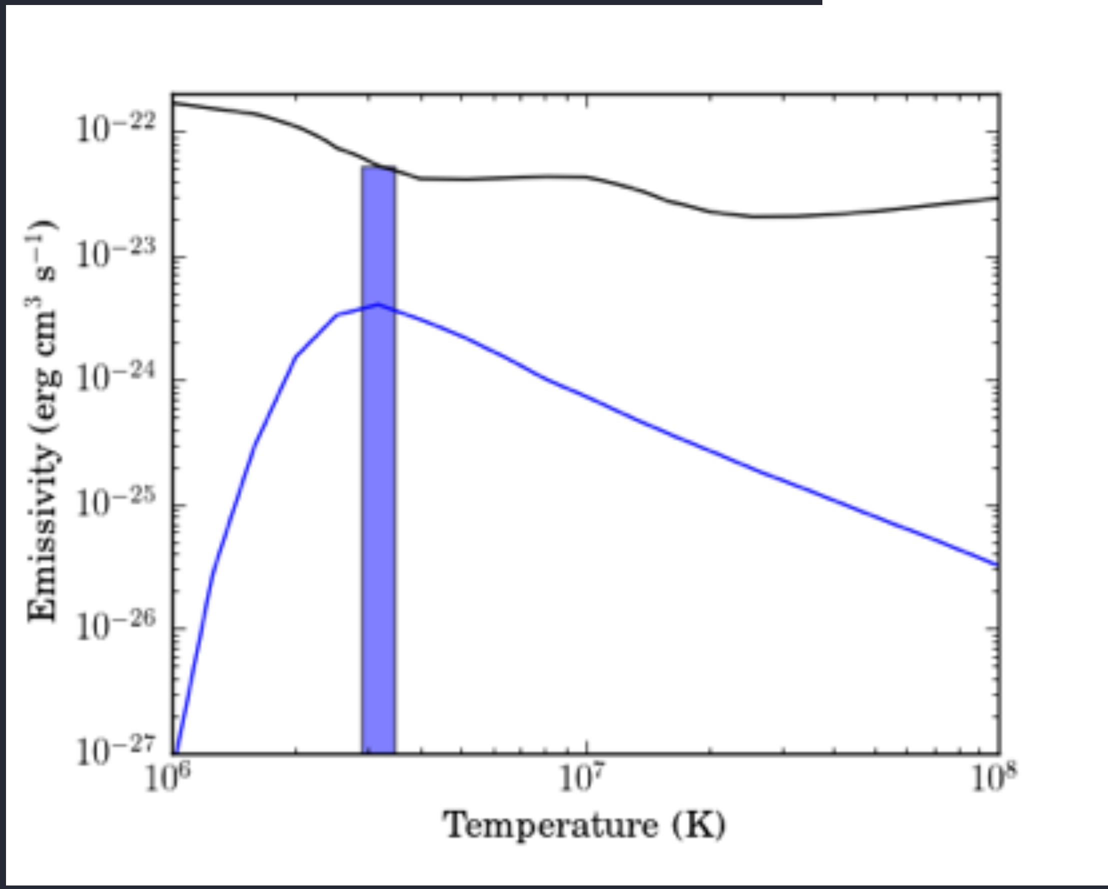

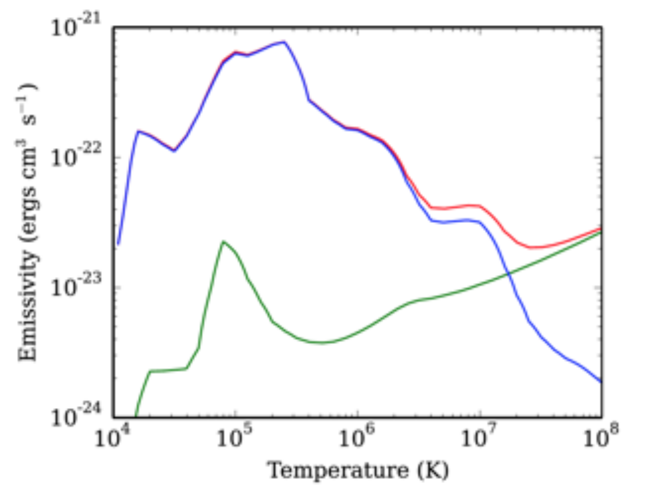

Figure 2. The contribution of all emission lines (blue) to the total radiated power (red), along with the contribution of continuum processes (green).

Not every shock is strong (hot) enough to produce radiation in a given line

L_{line} X-ray luminosity radiated into a *single line* as a shock cools:

$$L_\ell = \frac{\dot{M}}{\mu m_p}\frac{5}{2}k\Delta T_\ell \bar{N} p(T_\ell)$$

$p(T_{line})$, cumulative distribution of shock temperatures

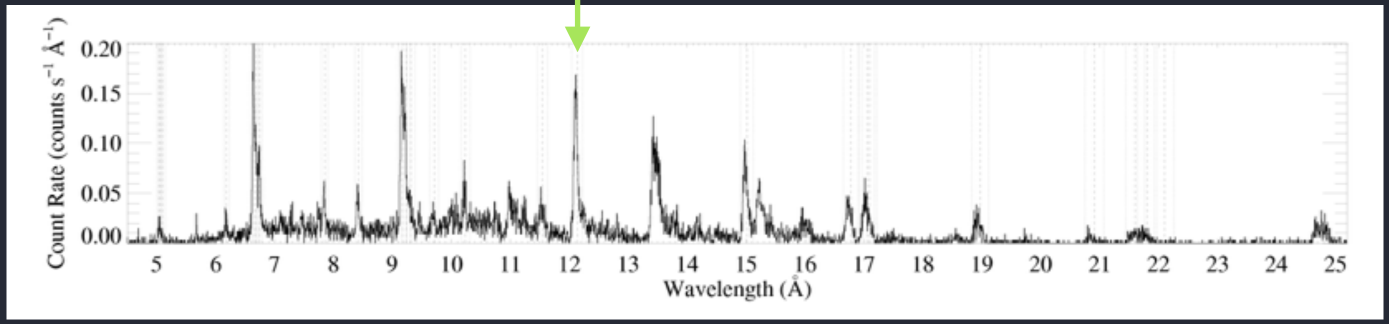

$p(T_{\rm line})$: probability that a shock heats the wind to temperature, $T_{\rm line}$, *or higher* (in which case the post-shock plasma will cool through $T_{\rm line}$)

correction for ISM attenuation

measured flux in an X-ray line

expectation value of the number of shocks a typical particle passes through that heat it to $T_{\rm line}$ or greater

$$L_\ell = 4\pi d^2 F_\ell e^{\tau_{\rm ism}} / T_{\rm w}(\tau_*)$$

correction for *wind* attenuation

$$\bar{N} p(T_\ell) = \frac{2\mu m_{\rm p} L_\ell}{5\dot{M} k \Delta T_\ell}$$

$$\Delta T_\ell \equiv \int_0^\infty \frac{\Lambda_\ell(T)}{\Lambda(T)}\, {\rm d}T$$

the temperature "equivalent width" - tabulated from atomic physics, ionization equilibrium (APEC)

$$L_\ell = 4\pi d^2 F_\ell e^{\tau_{\rm ism}} / T_{\rm w}(\tau_*)$$

correction for *wind* attenuation

Embedded Wind Shock (EWS) paradigm

Less than 1% of the mass of the wind is emitting X-rays

>99% of the wind is cold and X-ray *absorbing*

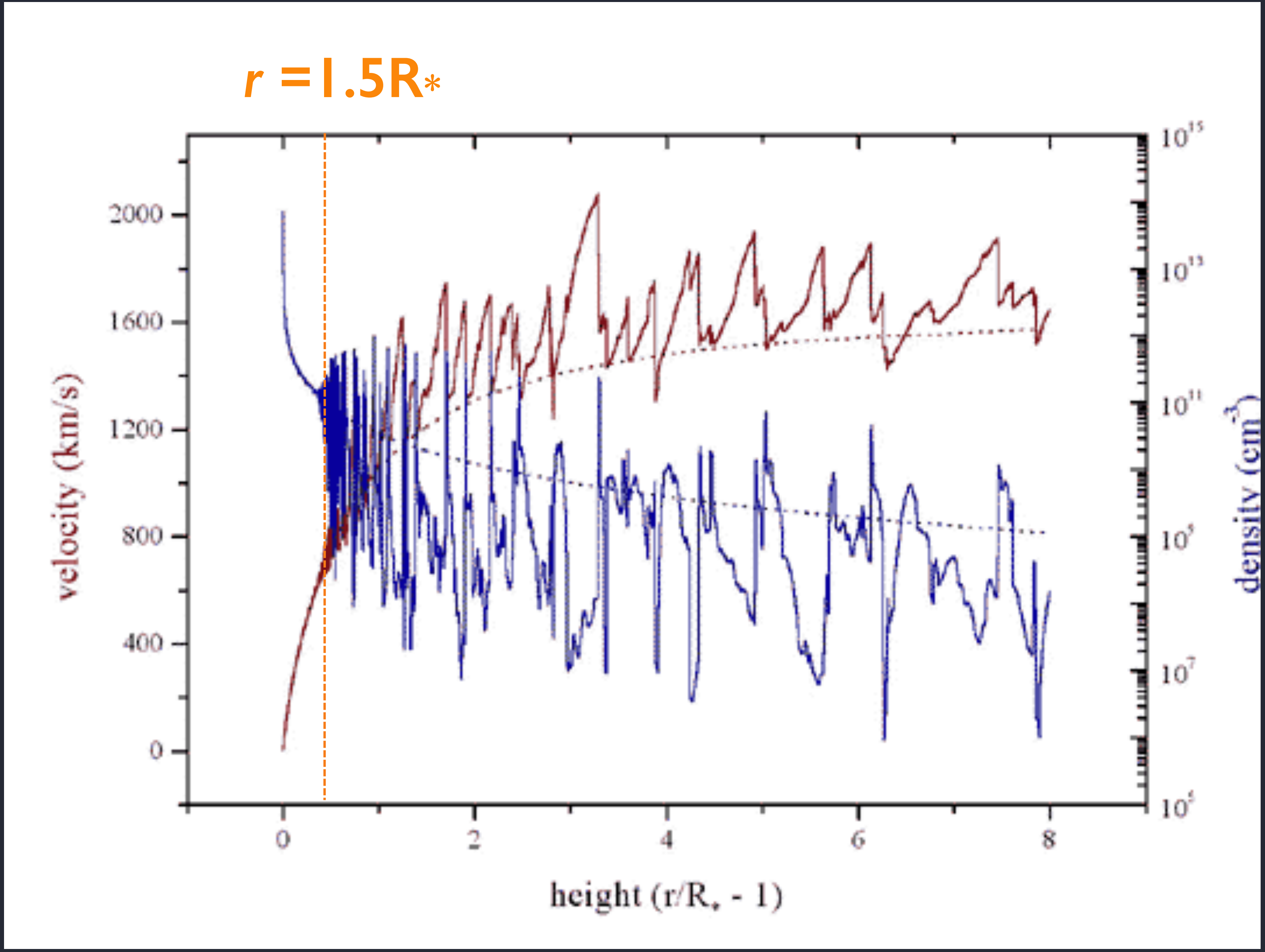

$$L_\ell = 4\pi d^2 F_\ell e^{\tau_{\rm ism}} / T_{\rm W}(\tau_*)$$

correction for *wind* attenuation

$$\tau(p, z, \lambda) = \int_z^\infty dz' \kappa(\lambda) \rho(r')$$

$$T(\tau_*) \equiv \frac{L_\lambda(\tau_*)}{L_\lambda(0)} = \frac{\int dV \rho^2 e^{-\tau}}{\int dV \rho^2}$$

THE ASTROPHYSICAL JOURNAL, 719:1767–1774, 2010 August 20 doi:10.1088/0004-637X/719/2/1767

MODELING BROADBAND X-RAY ABSORPTION OF MASSIVE STAR WINDS

MAURICE A. LEUTENEGGER[1,8], DAVID H. COHEN[2], JANOS ZSARGÓ[3,4], ERIN M. MARTELL[5,2], JAMES P. MACARTHUR[2], STANLEY P. OWOCKI[6], MARC GAGNÉ[7], AND D. JOHN HILLIER[4]
[1] Laboratory for High Energy Astrophysics, Code 662, NASA/Goddard Space Flight Center, Greenbelt, MD 20771, USA; Maurice.A.Leutenegger@nasa.gov
[2] Department of Physics and Astronomy, Swarthmore College, Swarthmore, PA 19081, USA
[3] Instituto Politecnico Nacional, Escuela Superior de Fisica y Matematicas, C.P. 07738, Mexico, D. F., Mexico
[4] Department of Physics and Astronomy, University of Pittsburgh, 3941 O'Hara Street, Pittsburgh, PA 15260, USA
[5] Department of Astronomy, University of Chicago, Chicago, IL 60637, USA
[6] Bartol Research Institute, University of Delaware, Newark, DE 19716, USA
[7] Department of Geology and Astronomy, West Chester University of Pennsylvania, West Chester, PA 19383, USA
Received 2010 April 16; accepted 2010 June 25; published 2010 August 3

Chandra grating spectra confirmed the EWS scenario

$v_{Doppler} \sim v_{wind}$

zeta Pup (O4 If): 63 ks *Chandra* MEG

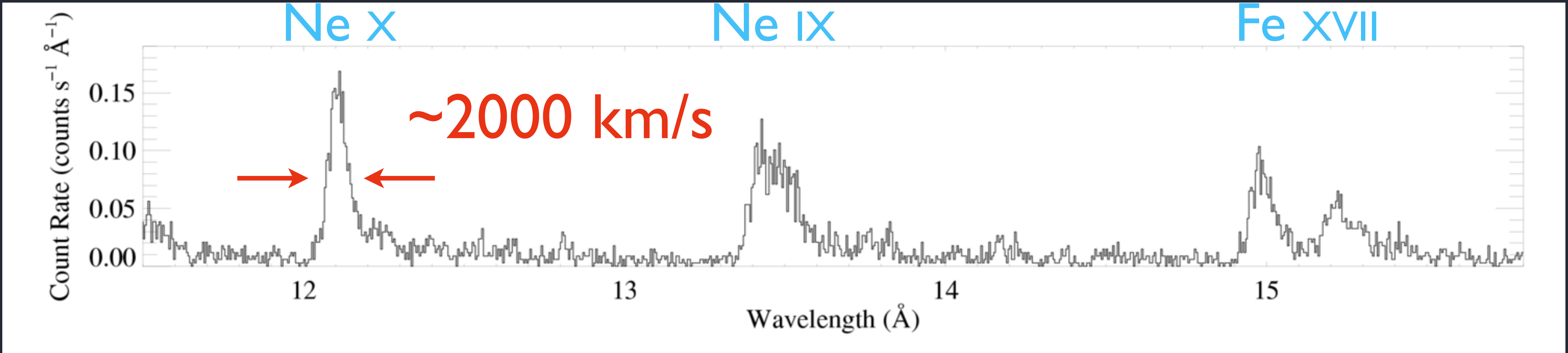

Chandra easily resolves the wind-broadened X-ray emission lines

lines are *asymmetric:*

this is a signature of wind absorption, and enables us to *measure the wind mass-loss rate*

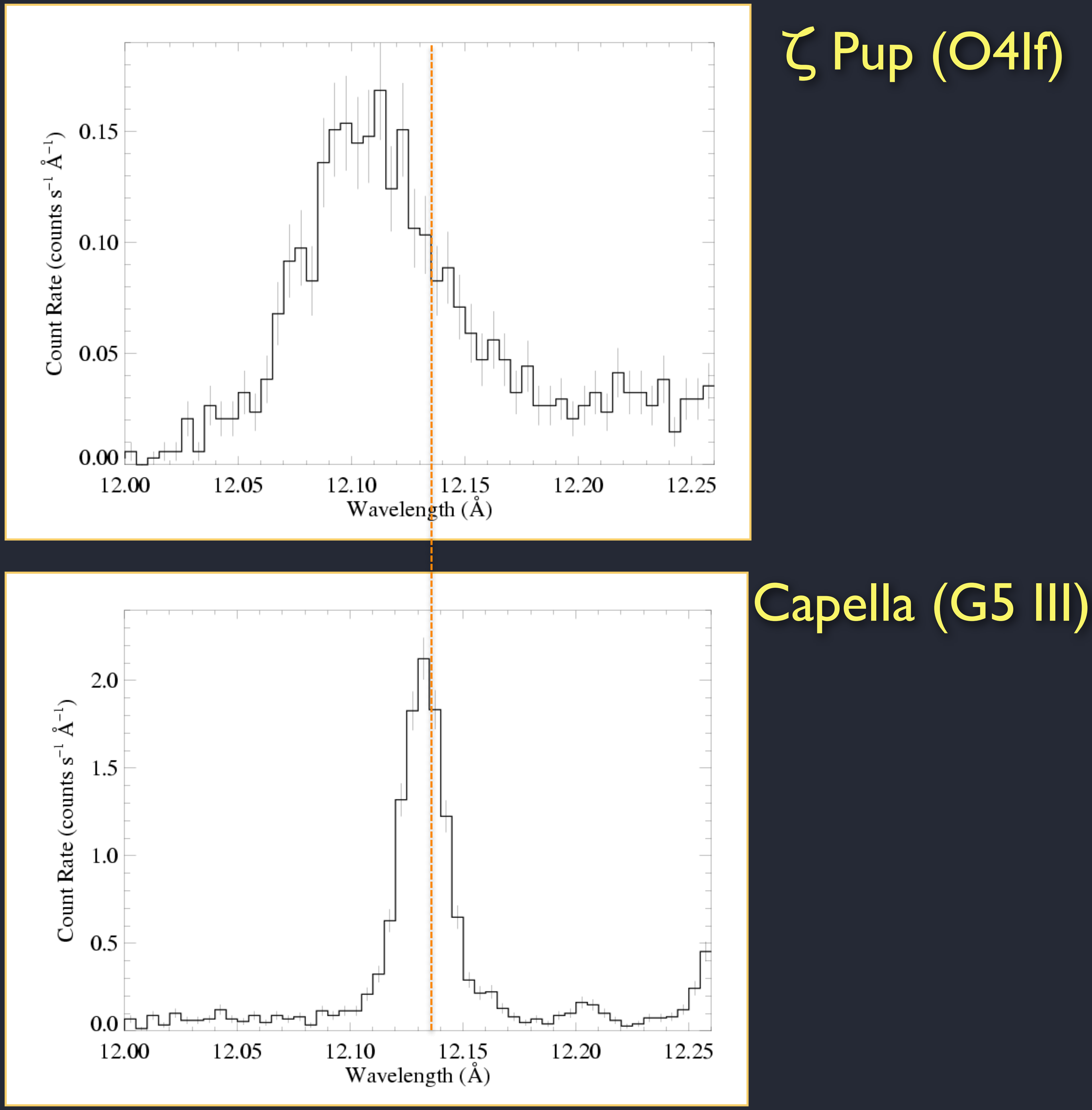

$v = v_\infty(1 - r/R_\star)^\beta$

beta velocity law assumed

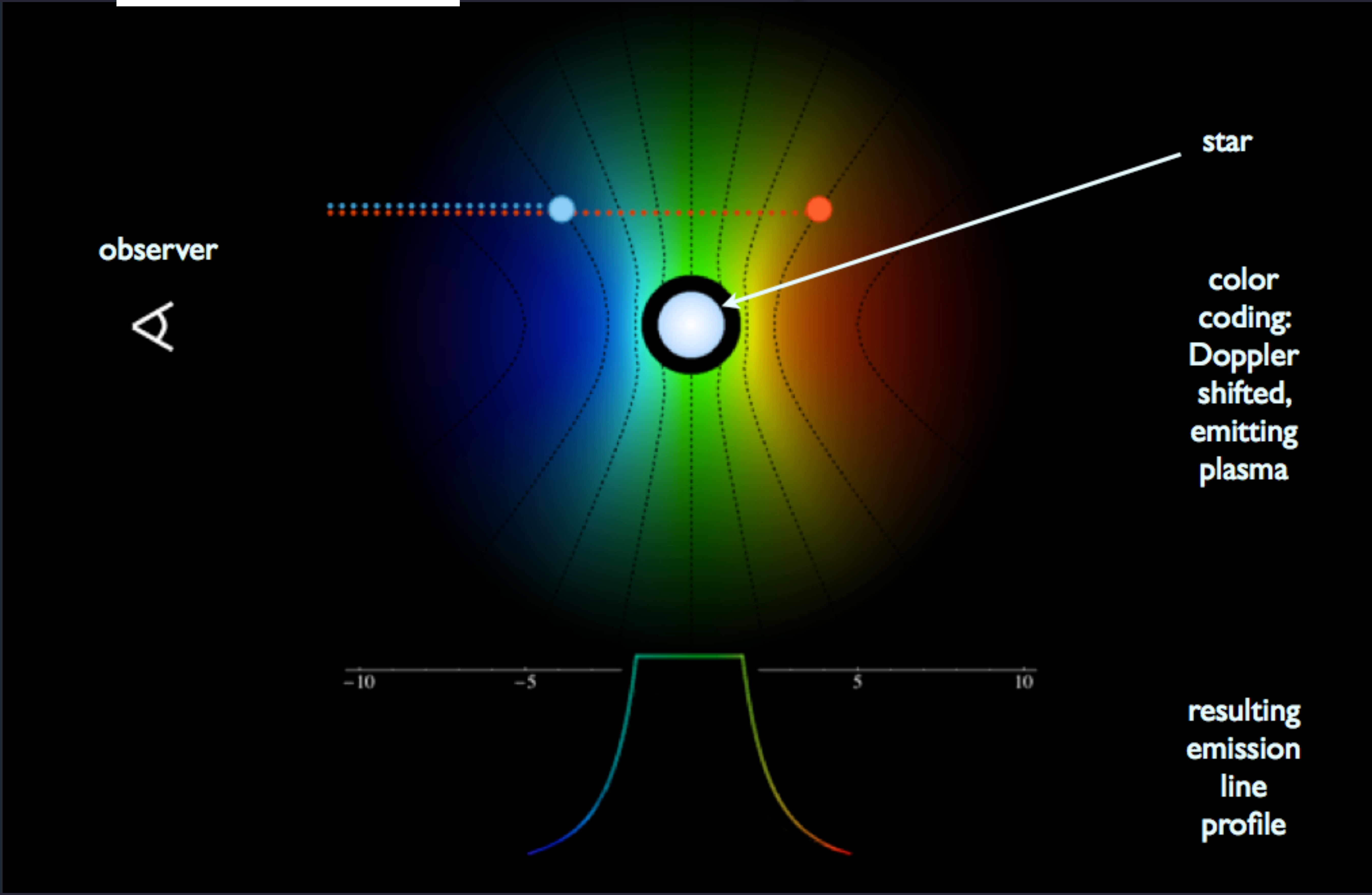

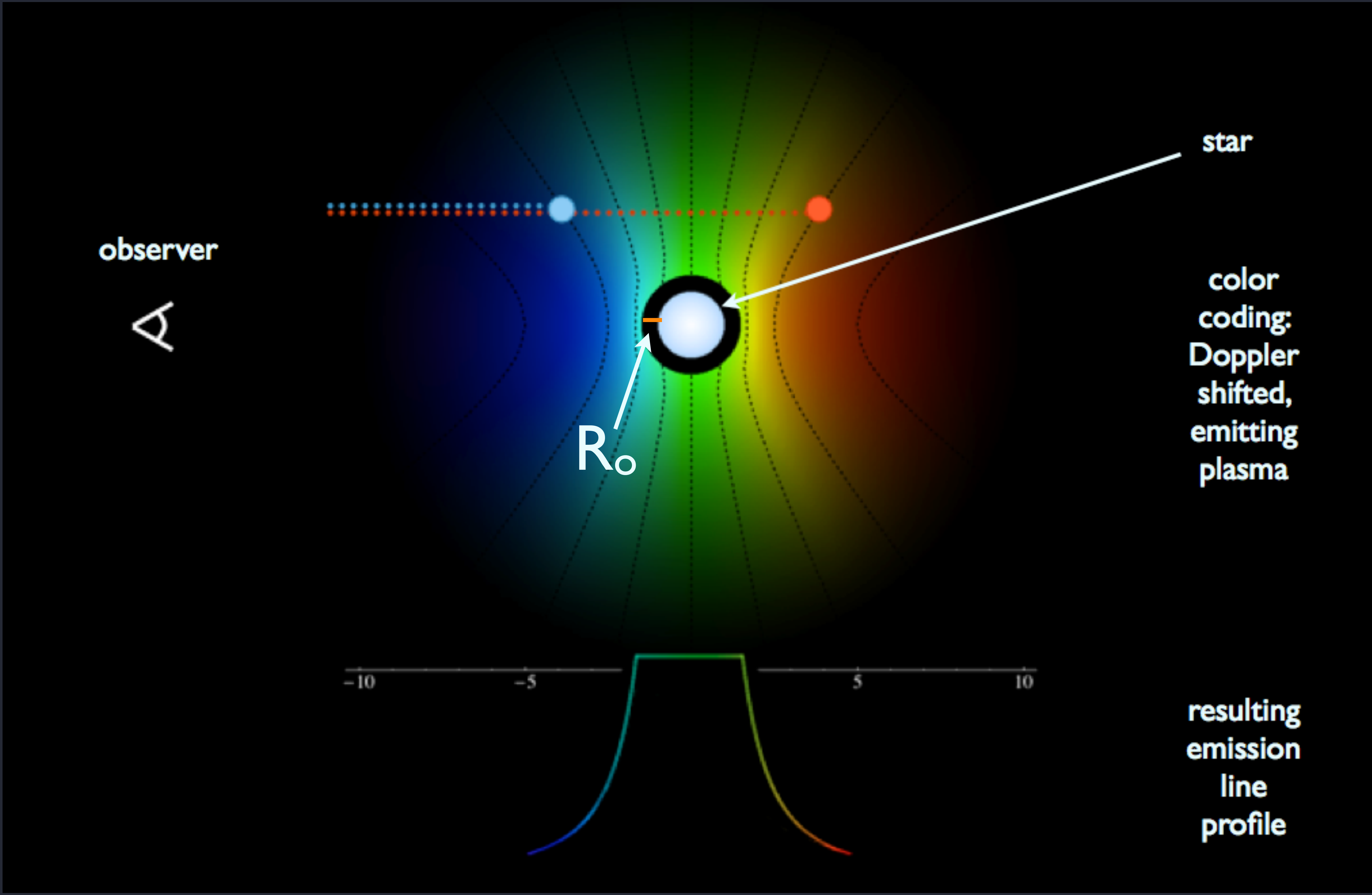

star
observer
color coding: Doppler shifted, emitting plasma
R○
−10
−5
5
10
resulting emission line profile

Line Asymmetry

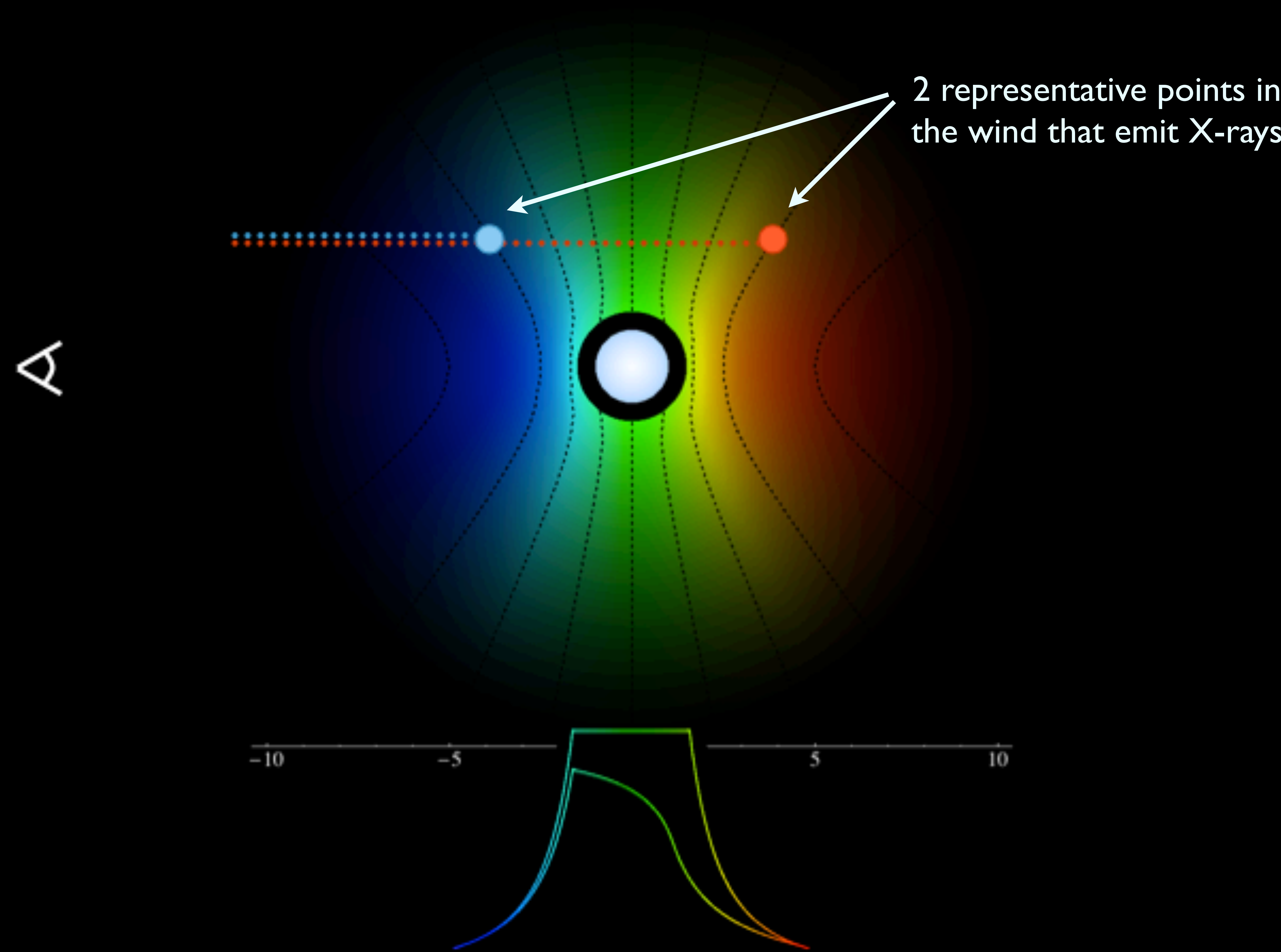

Line Asymmetry

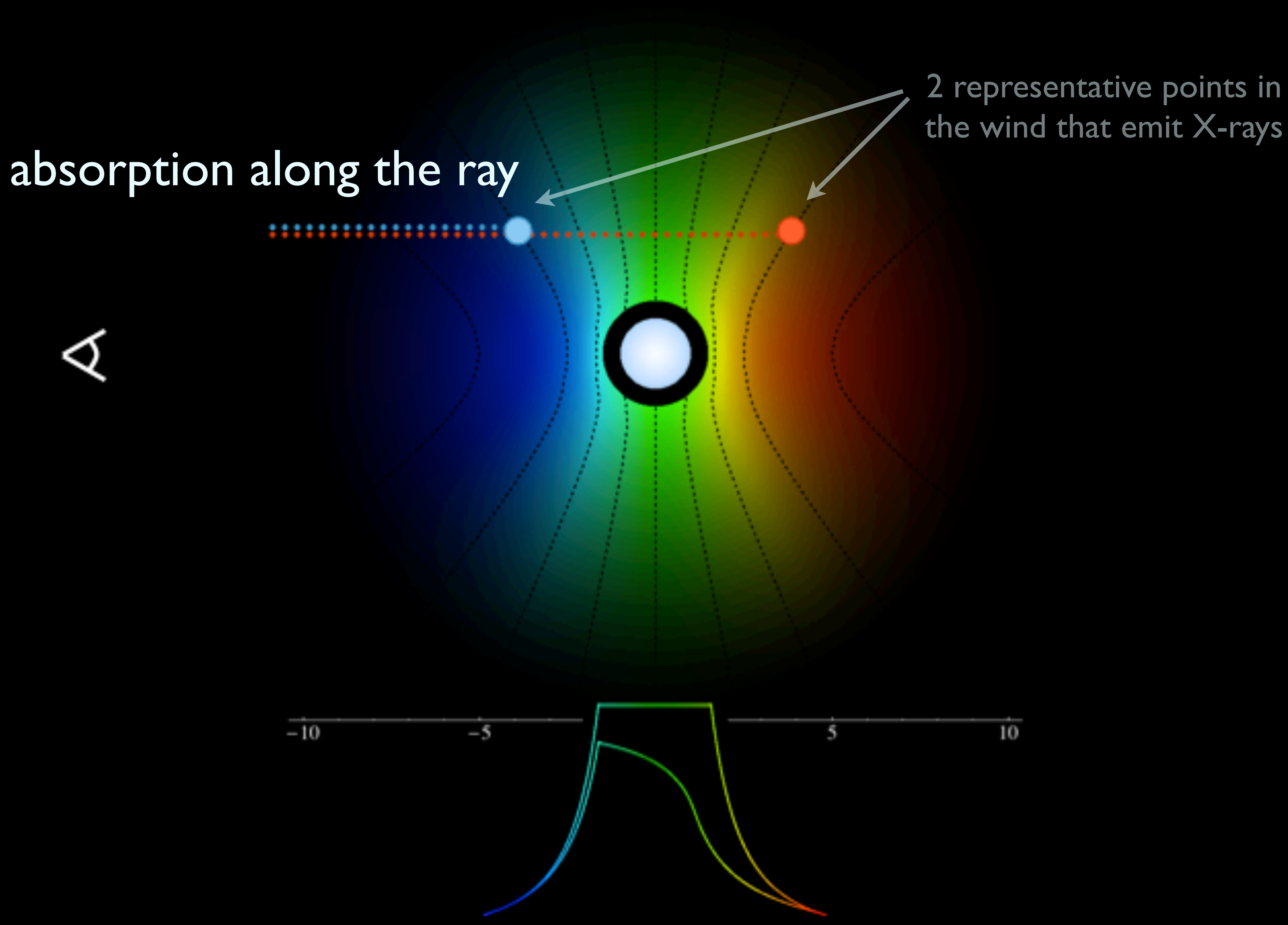

Line Asymmetry

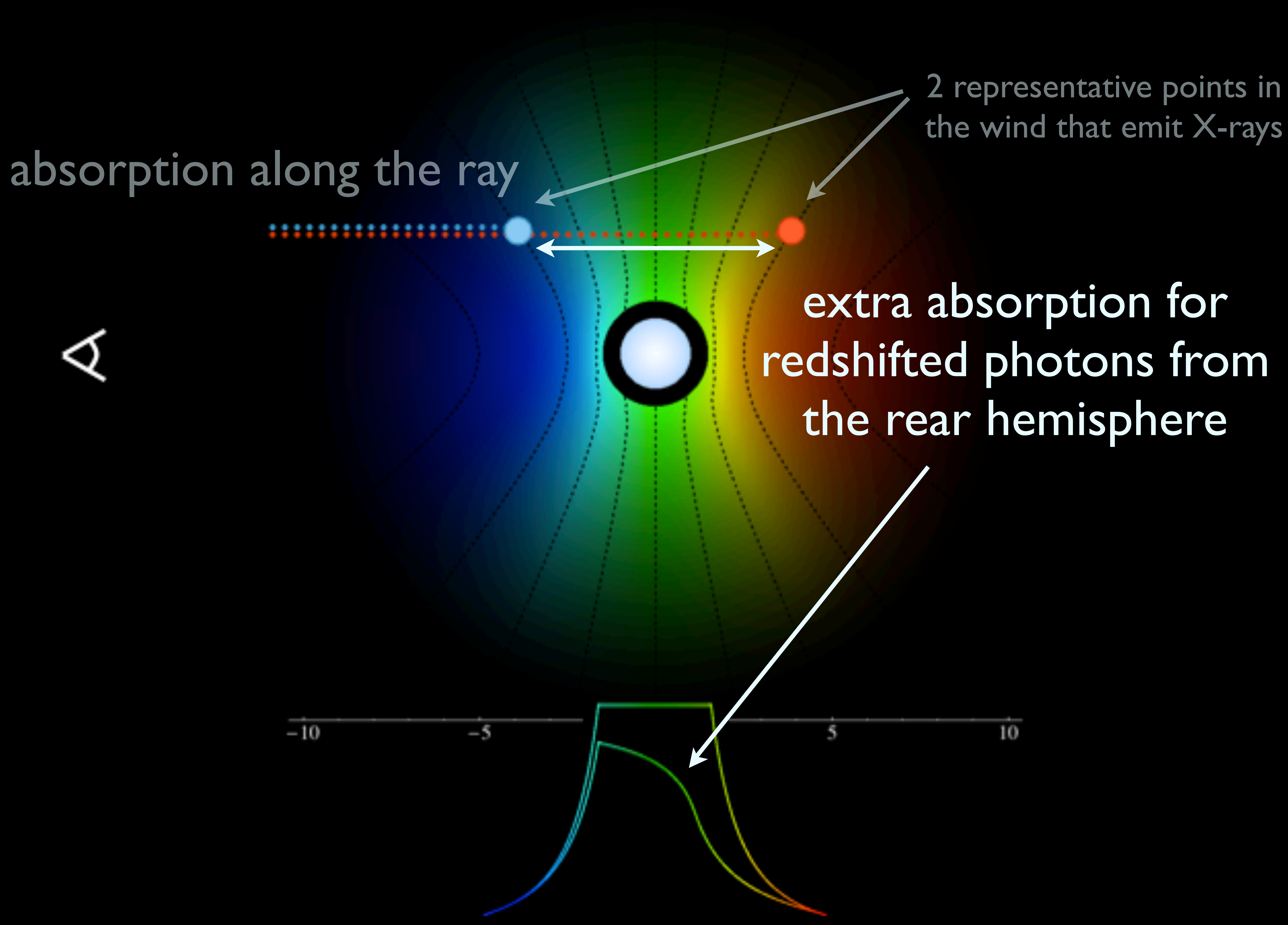

Wind Profile Model

mass-loss rates ~10^{-6}: expect wind to be modestly optically thick

$$\tau_* = \frac{\kappa \dot{M}}{4\pi R_* v_\infty}$$

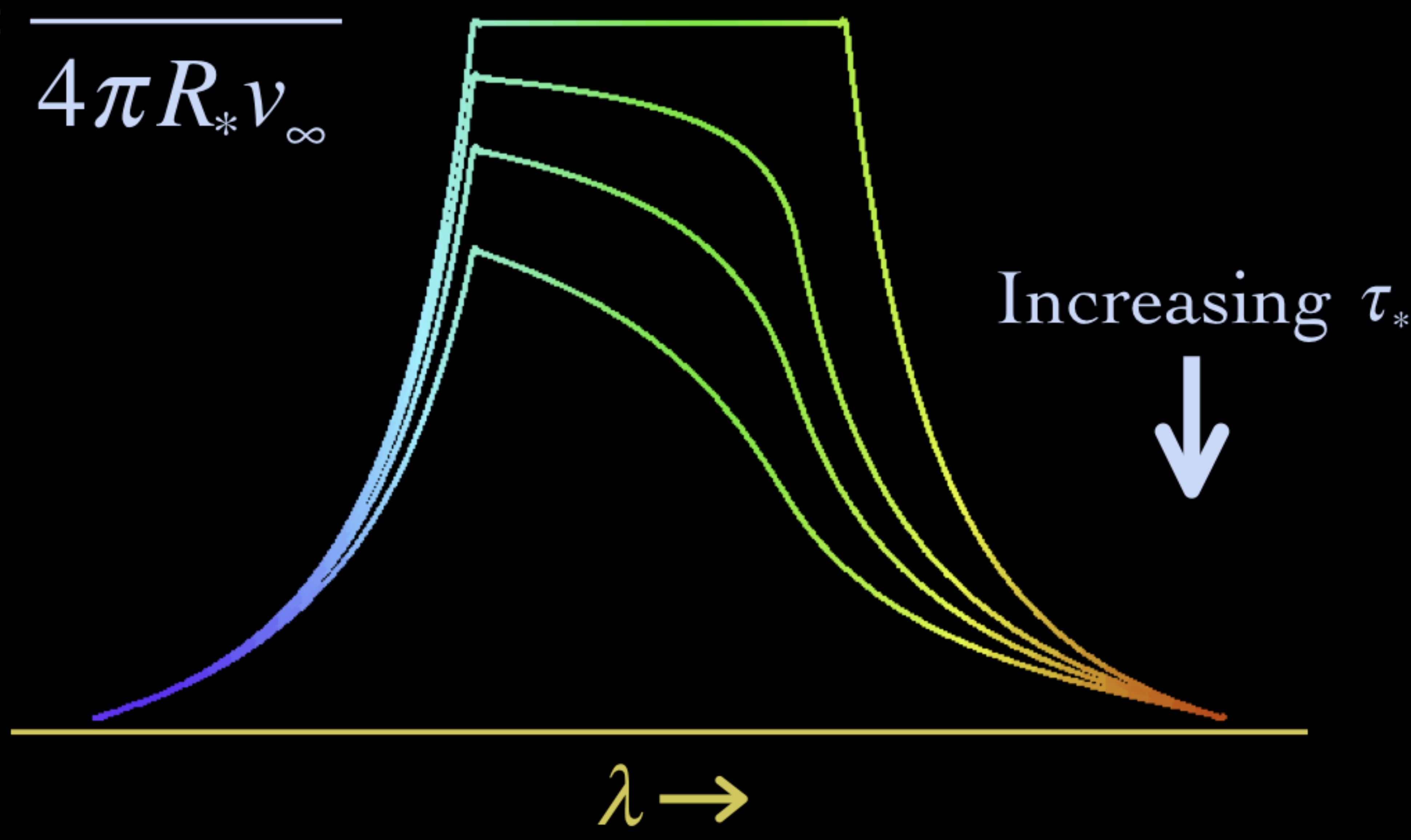

Line profile shapes

key parameters: R_o & $\tau_\star$

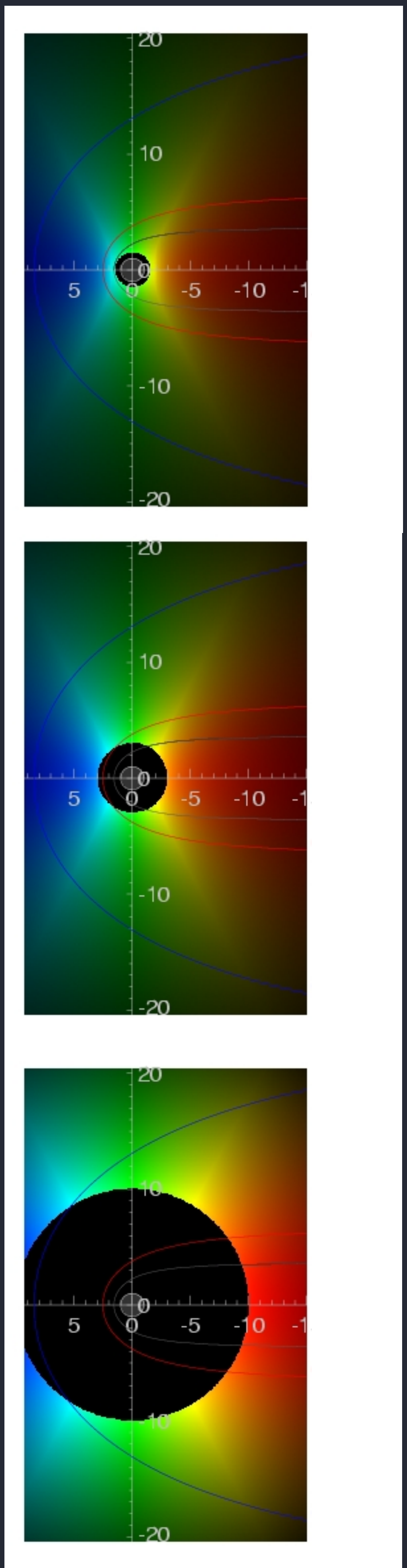

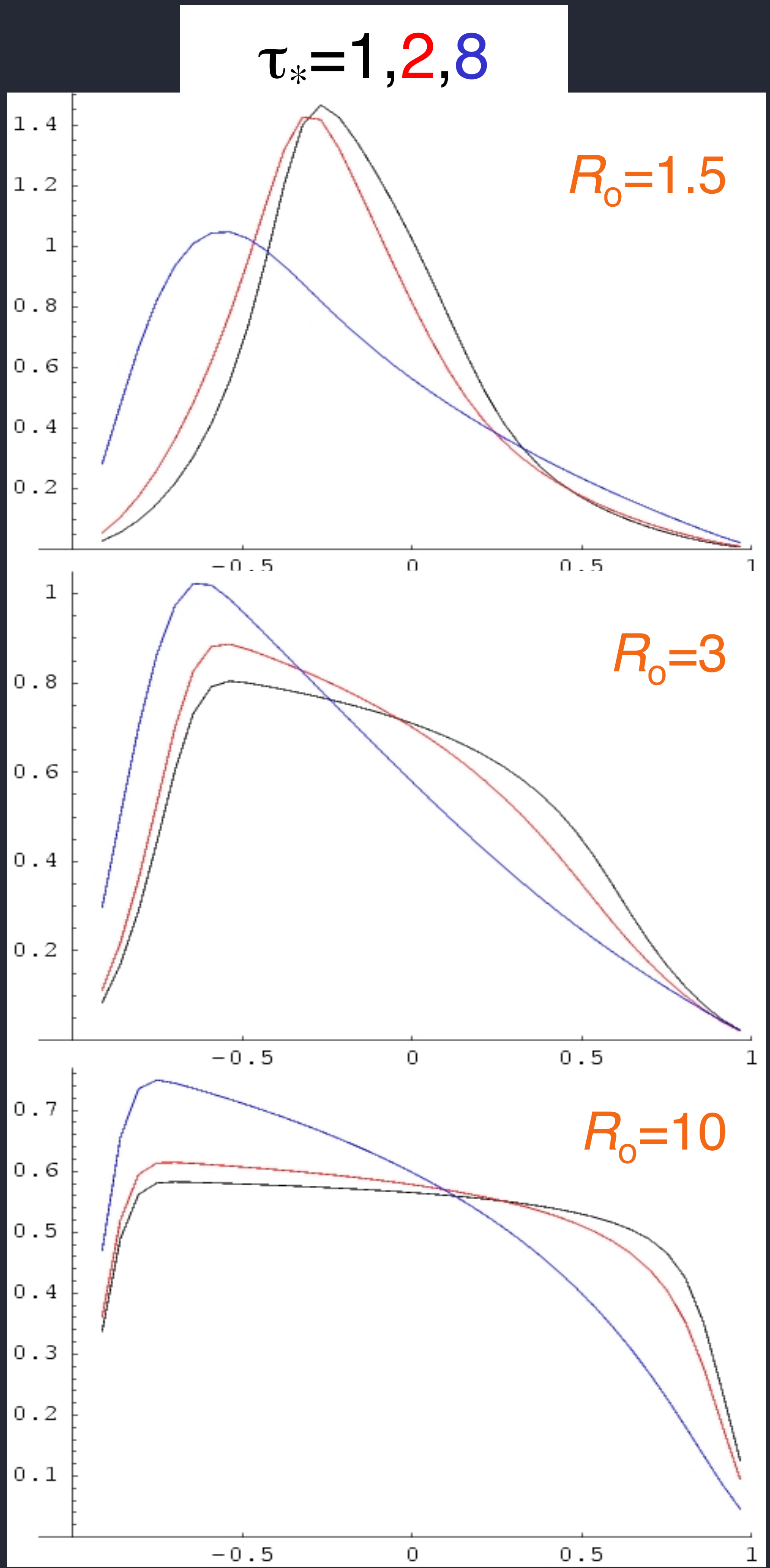

$$v = v_\infty (1 - r/R_\star)^\beta$$

$j \sim \rho^2$ for $r/R_* > R_o$,

$= 0$ otherwise

$$\tau = \tau_* \int_z^\infty \frac{R_* dz'}{r'^2 (1 - R_*/r')^\beta}$$

$$\tau_* \equiv \frac{\kappa \dot{M}}{4\pi R_* v_\infty}$$

Owocki & Cohen 2001

Fit the model to data

ζ Pup: *Chandra*

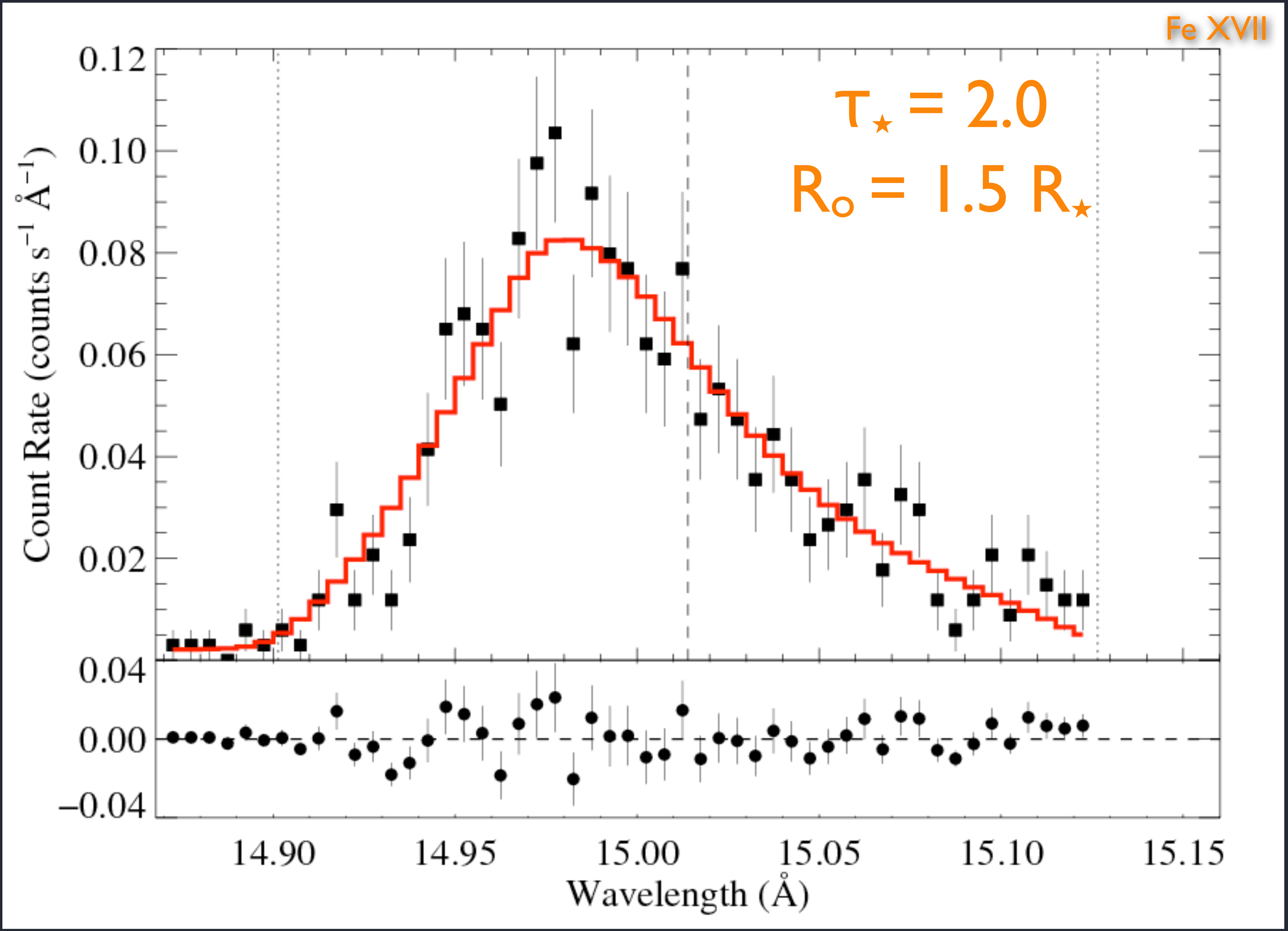

Apply a wind attenuation correction to each line in the *Chandra* spectrum

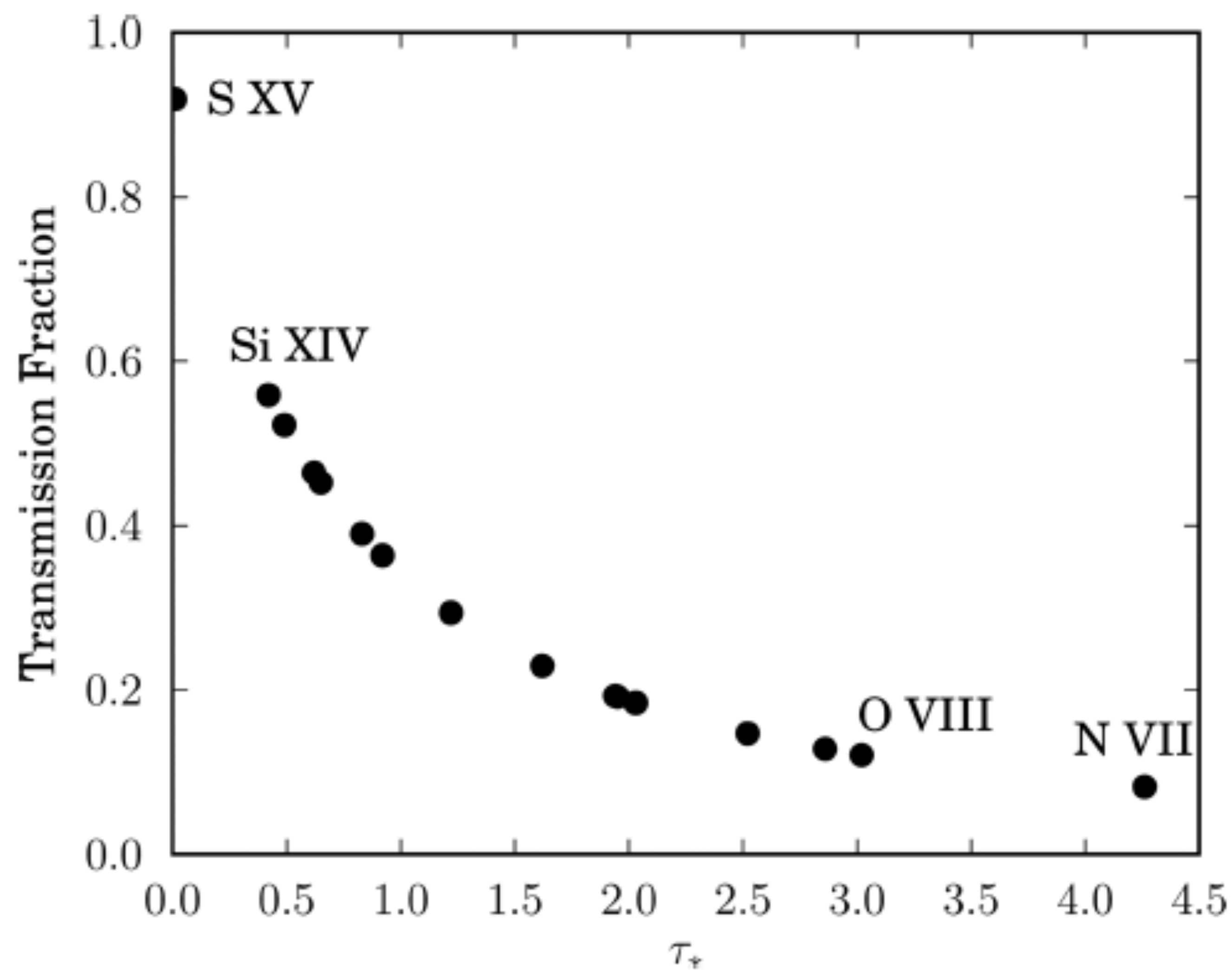

Figure 4. The fraction of the emitted line photons that are transmitted through the wind without being absorbed, for each line in the *Chandra* spectrum of ζ Pup, as a function of each line's characteristic optical depth value, τ_*, derived from fitting the line profile shapes (Cohen et al. 2014).

The attenuation corrections can be significant

and vary a lot from line to line

and they are *not* given by the simple exp(-tau) relationship.

correction for ISM attenuation

measured flux in an X-ray line

expectation value of the number of shocks a typical particle passes through that heat it to $T_{\rm line}$ or greater

$$L_\ell = 4\pi d^2 F_\ell e^{\tau_{\rm ism}} / T_{\rm w}(\tau_*)$$

correction for *wind* attenuation

$$\bar{N} p(T_\ell) = \frac{2\mu m_{\rm p} L_\ell}{5\dot{M} k \Delta T_\ell}$$

$$\Delta T_\ell \equiv \int_0^\infty \frac{\Lambda_\ell(T)}{\Lambda(T)}\, {\rm d}T$$

the temperature "equivalent width" - tabulated from atomic physics, ionization equilibrium (APEC)

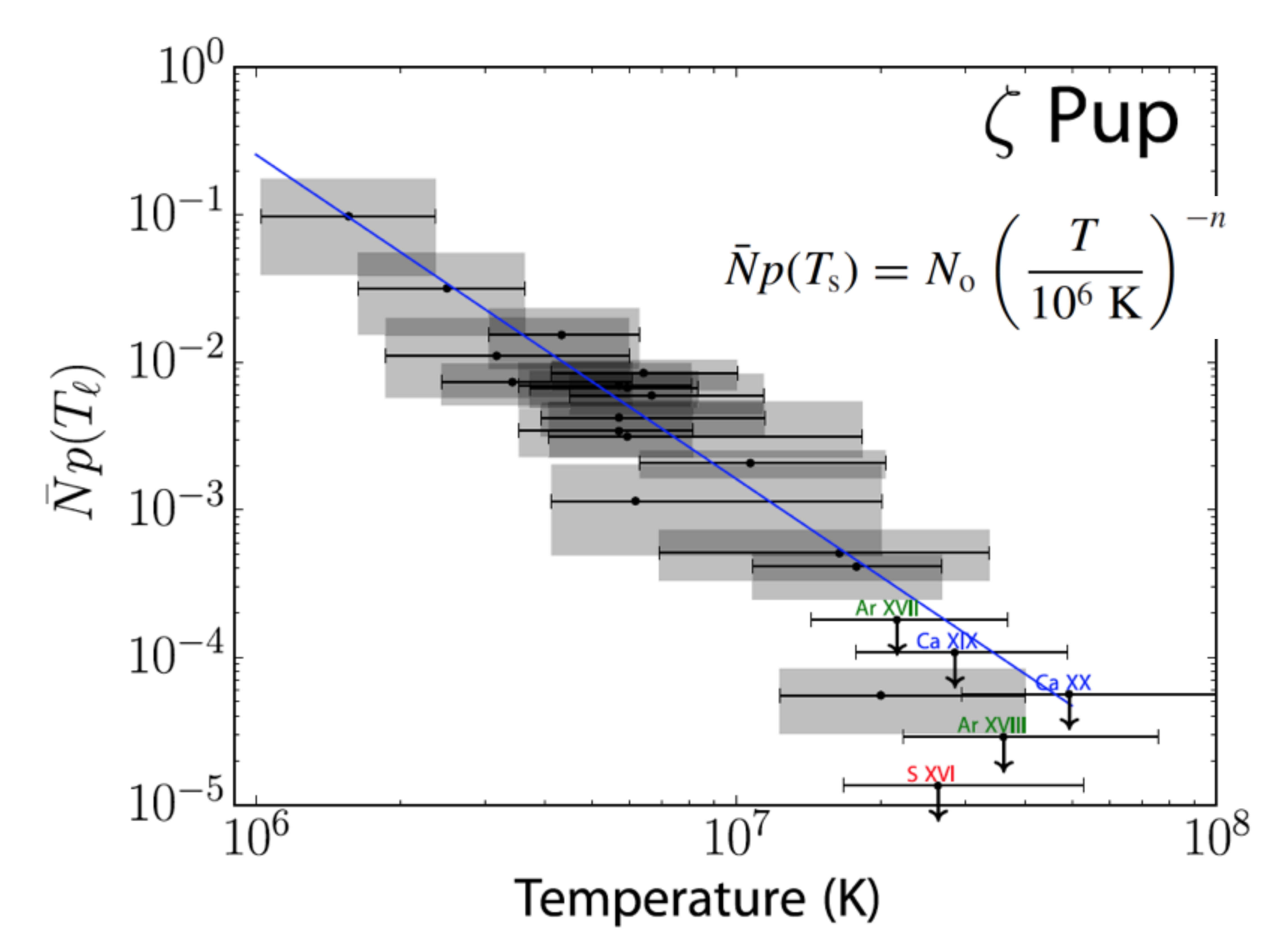

ζ Pup
$\bar{N}p(T_S) = N_o \left(\frac{T}{10^6\ K}\right)^{-n}$
$\bar{N}p(T_\ell)$
Temperature (K)
10^0
10^{-1}
10^{-2}
10^{-3}
10^{-4}
10^{-5}
10^6
10^7
10^8
Ar XVII
Ca XIX
Ca XX
Ar XVIII
S XVI

Five effectively single O stars with grating spectra in the *Chandra* archive

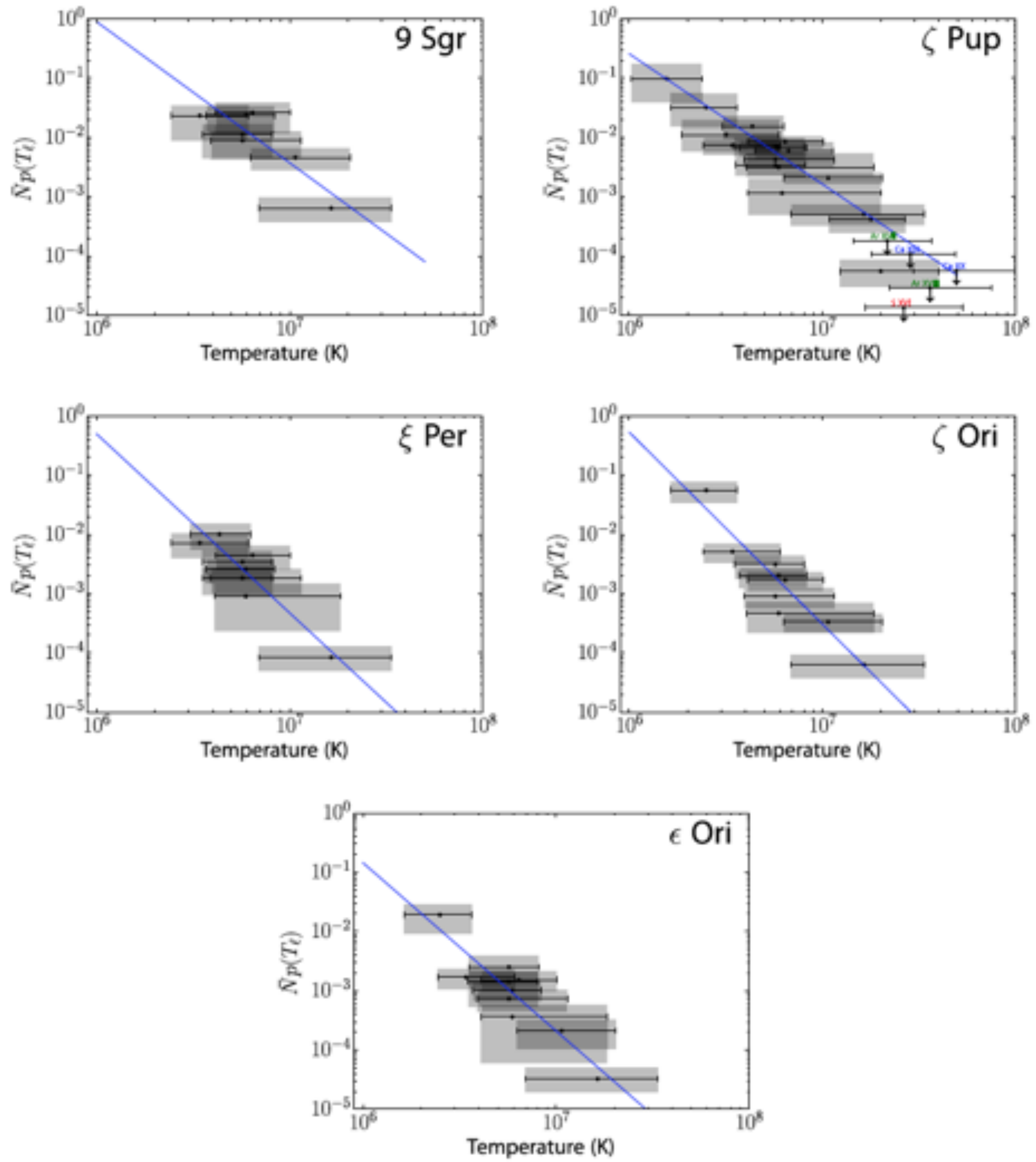

Figure 5. The shock-heating rate, $\dot{N}_P(T_\ell)$, is shown with the uncertainty on its value (vertical extent of each grey box) as well as the FWHM of the line emissivity ratio, $\Lambda_\ell(T)/\Lambda(T)$ (horizontal extent, visually reinforced by the horizontal error bars). The points are at T_ℓ for each line. The best-fitting power law to each set of values is shown as a blue line in each panel. For ζ Pup, the lowest temperature point corresponds to the N VI feature measured with *XMM–Newton*. And for this star, upper limits are included for five additional lines, none of which are detected in the *Chandra* spectrum.

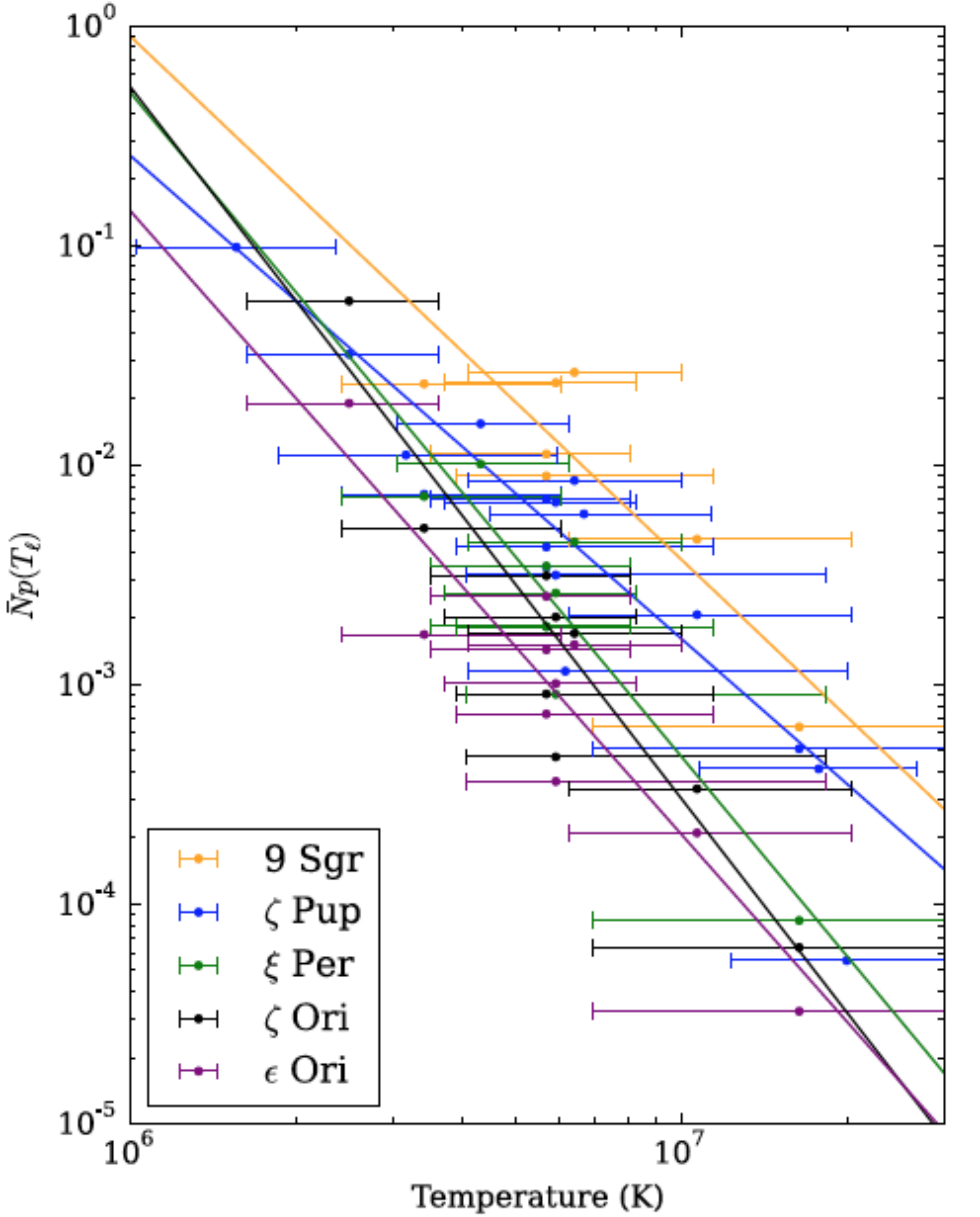

10^0
10^{-1}
10^{-2}
10^{-3}
10^{-4}
10^{-5}
$\bar{N}p(T_\ell)$
10^6
10^7
Temperature (K)
9 Sgr
ζ Pup
ξ Per
ζ Ori
ϵ Ori

$N_o \sim 0.1$ to 1
$n \sim 2$ to 3

Table 2. Power-law fits to $\bar{N}p(T_\ell)$ values.

Star	Spectral Type	N_o	n
9 Sgr	O4 V	0.90	2.38
ζ Pup	O4 If	0.26	2.20
ξ Per	O7.5 III	0.50	3.02
ζ Ori	O9.7 Ib	0.53	3.24
ϵ Ori	B0 Ia	0.14	2.84

$\bar{N}p(T_\ell)$

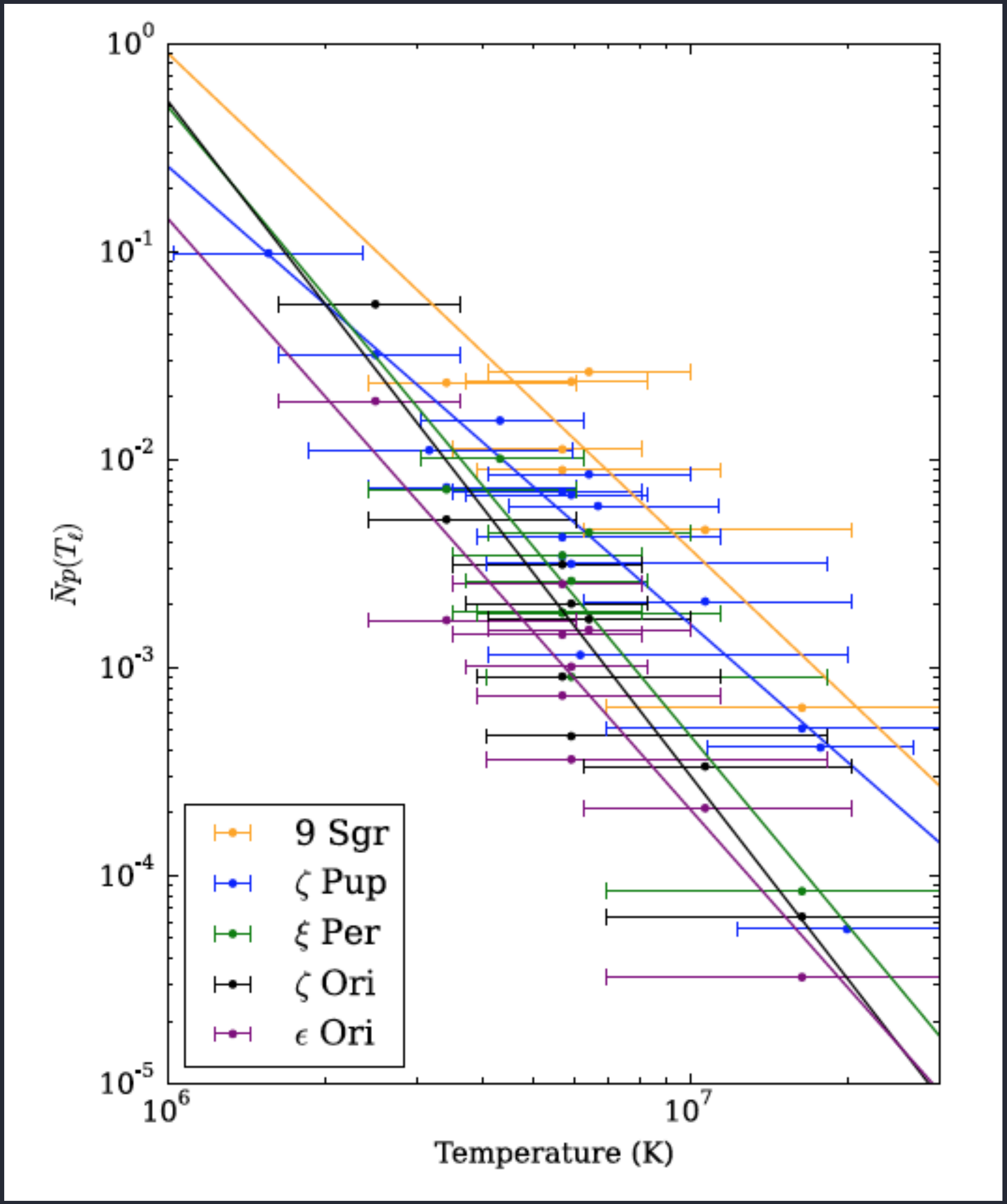

Table 2. Power-law fits to $\bar{N}p(T_\ell)$ values.

Star	Spectral Type	N_o	n
9 Sgr	O4 V	0.90	2.38
ζ Pup	O4 If	0.26	2.20
ξ Per	O7.5 III	0.50	3.02
ζ Ori	O9.7 Ib	0.53	3.24
ϵ Ori	B0 Ia	0.14	2.84

Turn-over or cut-off at high temperatures?

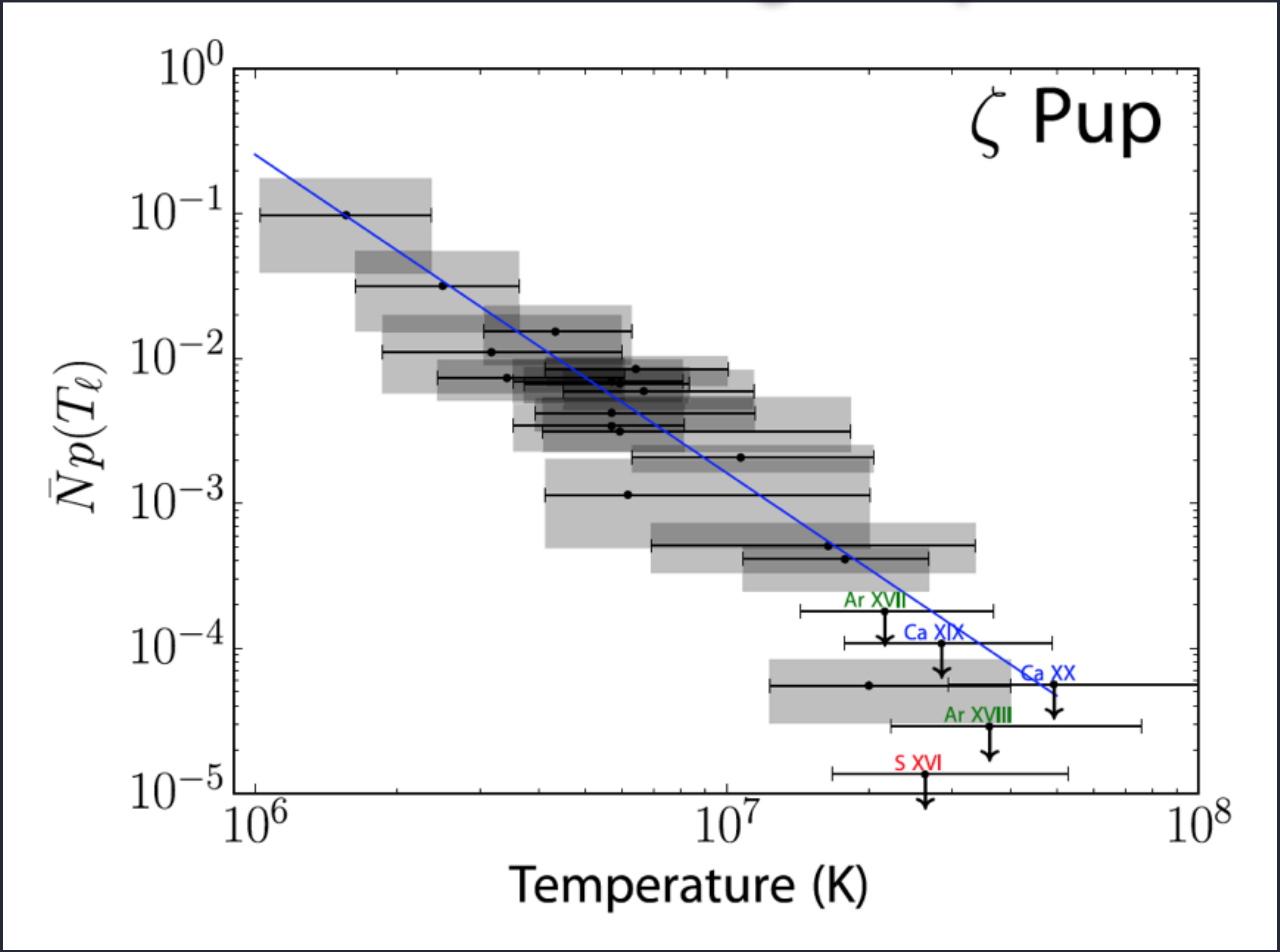

Observation constraints on theory/ simulations

Track parcels as they flow through the wind; discontinuities are shocks

$T_{shock} = 10^6\ (v_{shock}/270\ \text{km/s})^2\ \text{K}$

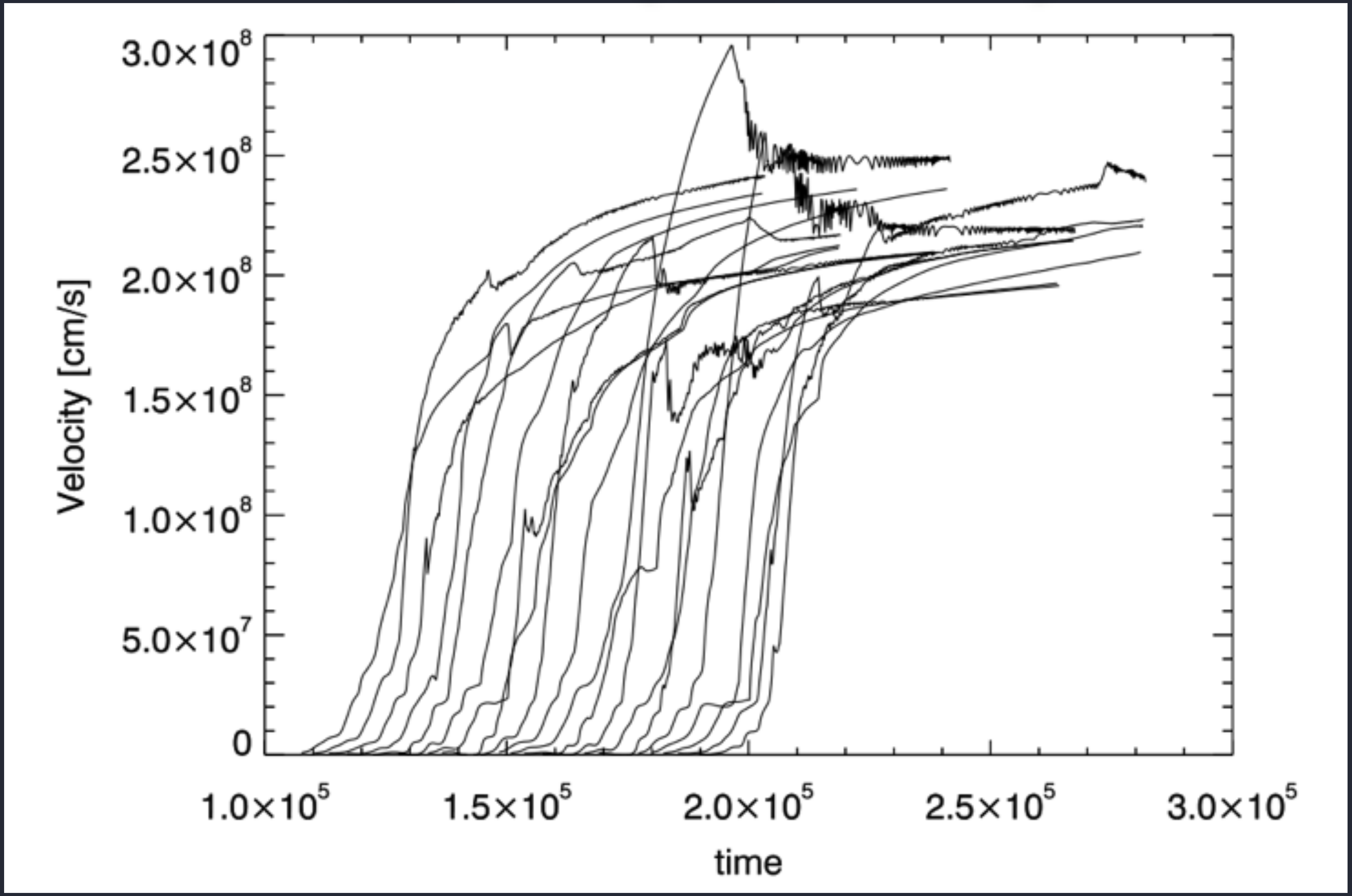

Observation constraints on theory/simulations

from 1-D numerical simulations

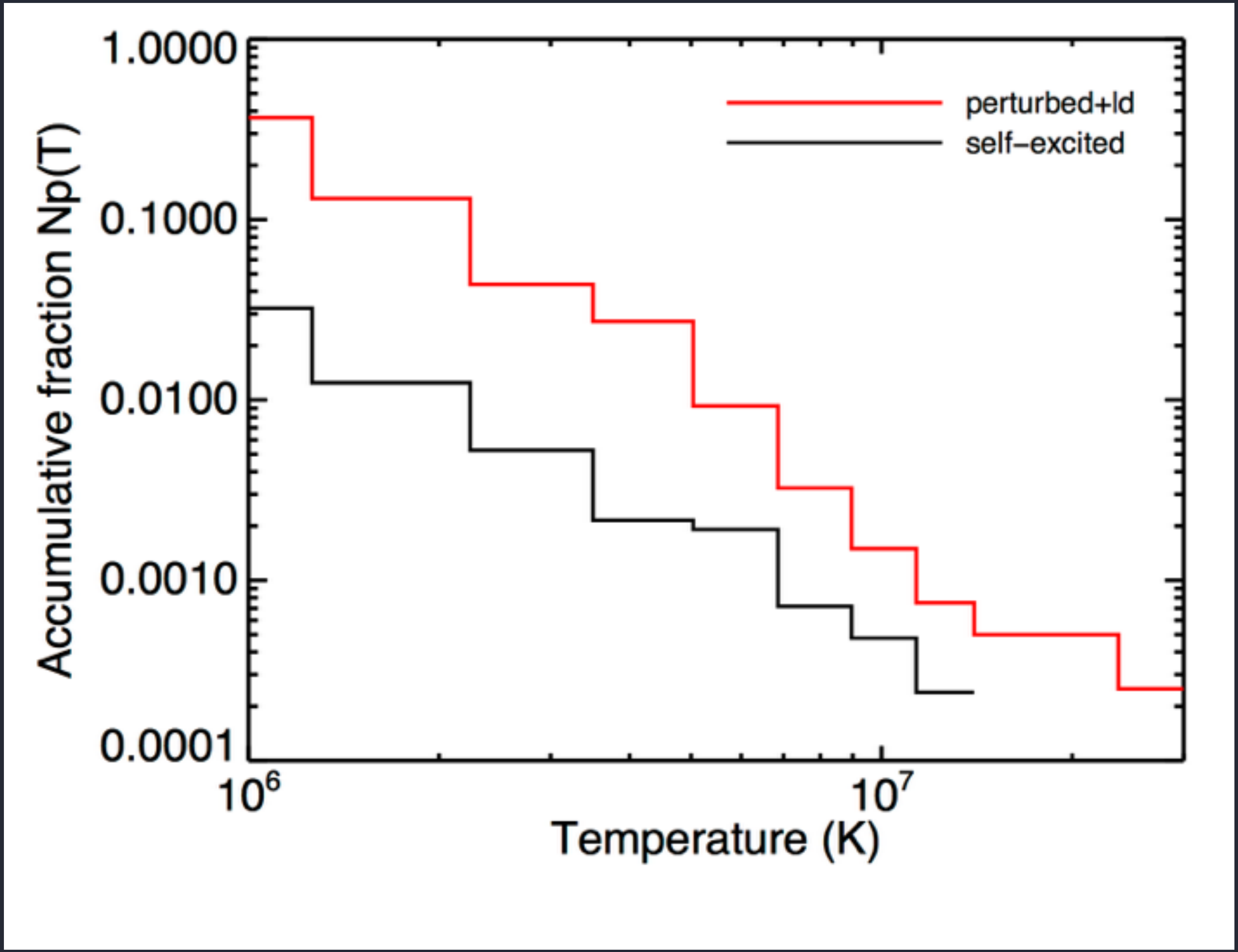

Observation constraints on theory/ simulations

from 1-D numerical simulations

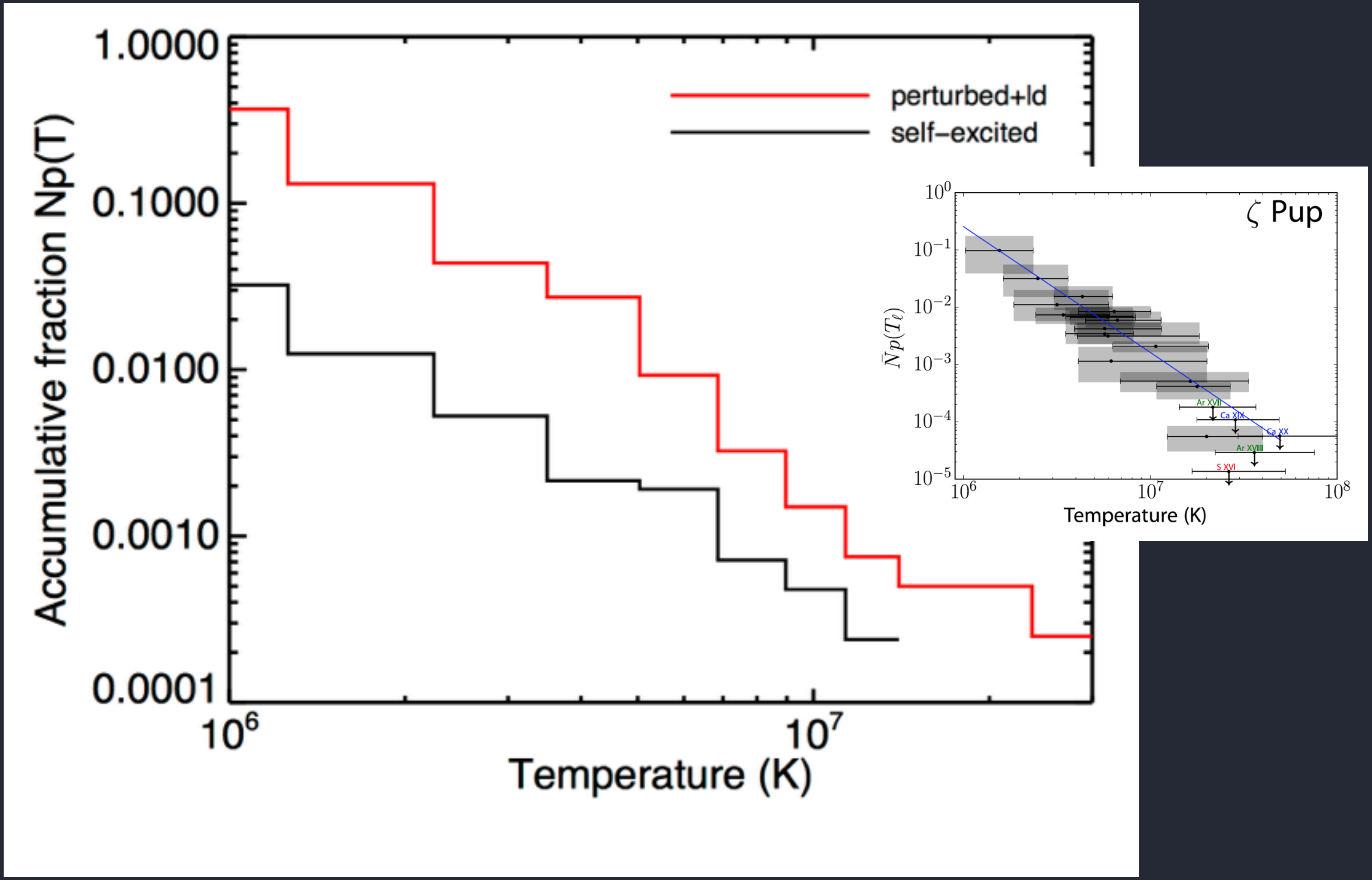

Theory/simulation issues

Line force cut-off for most optically thick lines (numerical issues)

Lower boundary conditions: self-excited vs. perturbed; also limb darkening - role of clump-clump collisions

Multi-dimensional effects

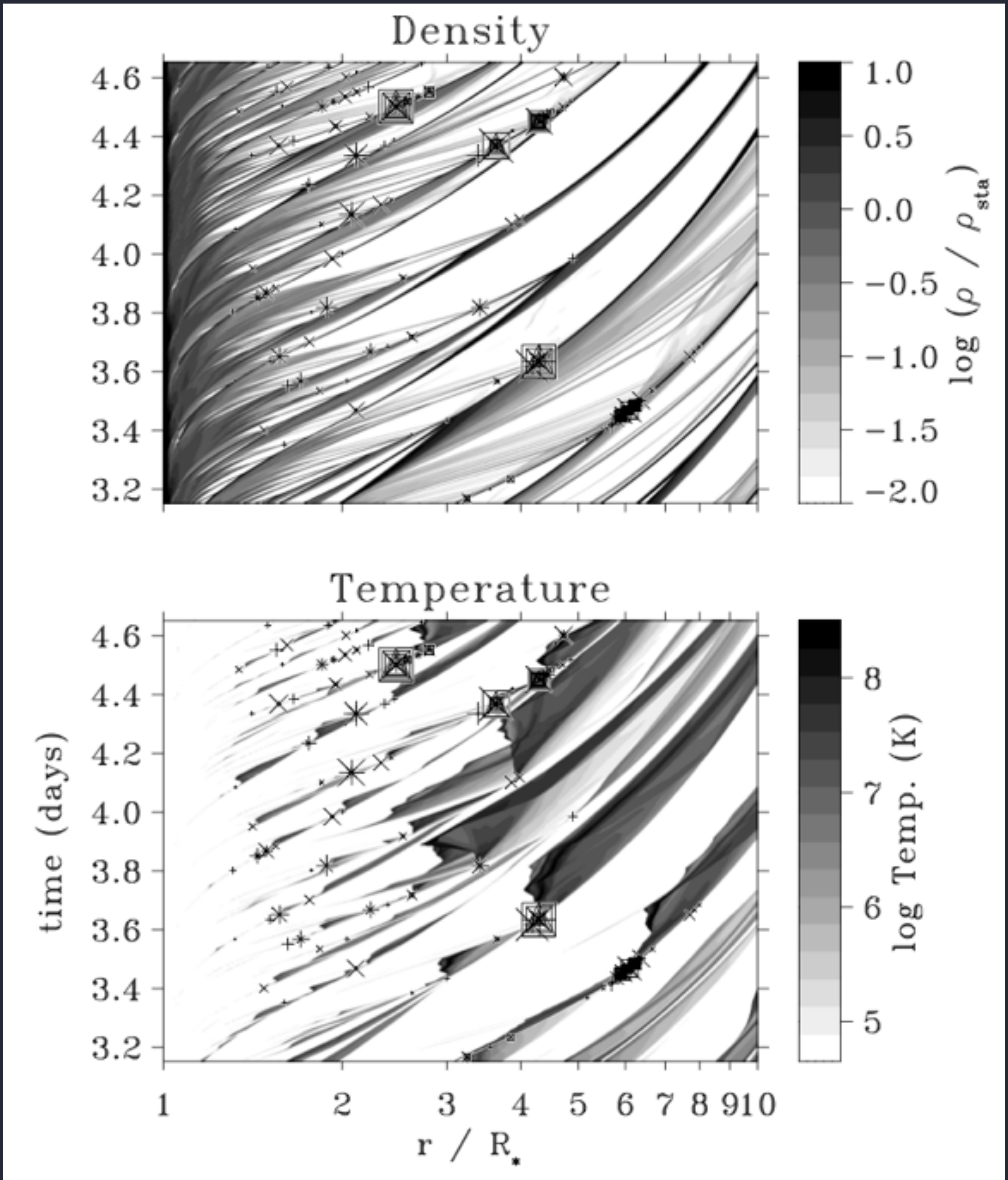

Feldmeier, Puls, & Pauldrach (1997)

clump-clump collisions
- what about 2-D? 3-D?

Lower boundary conditions

self-excited

photospheric perturbations +
limb darkening

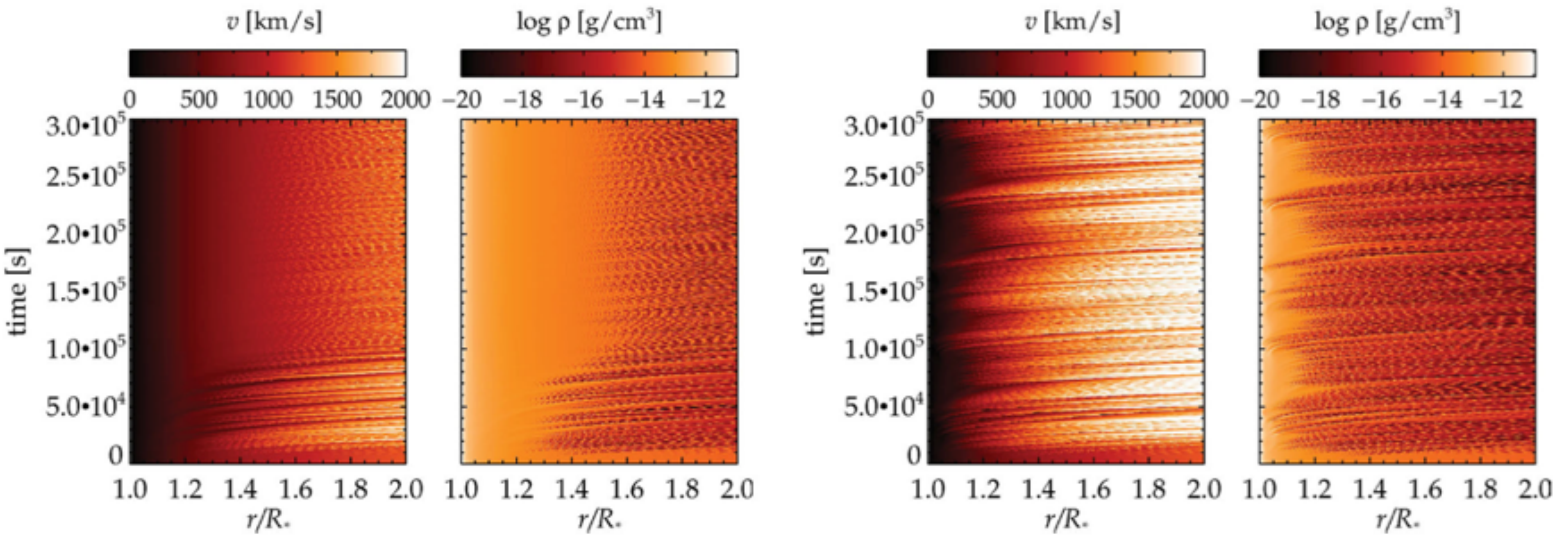

Figure 4. Inner wind time evolutions of a simulation without limb darkening and photospheric perturbations (left) and one including both effects (right).

Conclusions

impulsive heating with radiative cooling enables a simple correction for the cooling and the extraction of the impulsive heating rate and temperature distribution

EWS in O stars generate a relatively universal heating distribution: wind material undergoes roughly one shock, and strong shocks are much less commonly produced than weak ones

The rate seems to decline very sharply above 10^7 K